frontiers | Frontiers in Environmental Science

TYPE Original Research
PUBLISHED 26 September 2025
DOI 10.3389/fenvs.2025.1668462

OPEN ACCESS

EDITED BY
Paula S Tourinho,
Masaryk University, Czechia

REVIEWED BY
Nirosha Ruwani Amarasekara,
Agricultural Research Service (USDA),
United States
Sunita Singh,
DY Patil Deemed to be University, India

*CORRESPONDENCE
Philips O. Akinwole,
philipsakinwole@depauw.edu

†PRESENT ADDRESS
Emma E. C. Jacobs,
Ecology and Evolutionary Biology Department,
Tulane University, New Orleans, LA,
United States
Nina G. Shaffer,
Plant and Soil Sciences Department, University
of Kentucky, Lexington, KY, United States

RECEIVED 25 July 2025
ACCEPTED 15 September 2025
PUBLISHED 26 September 2025

CITATION
Akinwole PO, Jacobs EEC and Shaffer NG (2025) Carbon metabolism and multidrug resistance in *Bacillus mobilis* and *Cupriavidus campinensis* isolated from cadmium-spiked soils.
Front. Environ. Sci. 13:1668462.
doi: 10.3389/fenvs.2025.1668462

Carbon metabolism and multidrug resistance in *Bacillus mobilis* and *Cupriavidus campinensis* isolated from cadmium-spiked soils

Philips O. Akinwole*, Emma E. C. Jacobs† and Nina G. Shaffer†

Biology Department, DePauw University, Greencastle, IN, United States

Heavy metal contamination and antibiotic resistance are critical environmental and public health challenges, often exacerbated by co-selection pressures in polluted environments. This study identifies and characterizes *Bacillus mobilis and Cupriavidus campinensis*, two cadmium-tolerant bacterial species isolated from cadmium-amended soils with cadmium (Cd^{2+}) concentrations exceeding those typically found in highly contaminated soils. Both species exhibited multidrug resistance and the ability to metabolize specific carbon substrates, including pyruvic acid methyl ester, itaconic acid, D-galactonic acid-γ-lactone, Tween-40, and Tween-80. These substrates enhance microbial activity and heavy metal bioavailability, supporting their potential roles in bioremediation, especially through the targeted introduction of optimal carbon substrates. Antibiotic susceptibility testing revealed distinct growth dynamics under exposure to antibiotics such as ceftriaxone, ciprofloxacin, gentamicin, and tetracycline. Notably, *C. campinensis* displayed extended lag phases and concentration-dependent growth inhibition, with delayed recovery observed for ceftriaxone and doripenem. In contrast, *B. mobilis* exhibited resistance to several antibiotics, including erythromycin and vancomycin, and adaptive responses to ciprofloxacin, levofloxacin and nitrofurantoin, suggesting robust resistance mechanisms. These findings highlight the limitations of standard 24-h testing protocols, which fail to capture delayed adaptive responses critical for understanding resistance in complex environments. *In silico* resistome profiling of the isolates confirmed high-risk resistance genes, including β-lactamases (*blaZ*, *mecA*), fluoroquinolone targets (*gyrA*, *parC*), macrolide resistance genes (*ermB*, *ermC*), and tetracycline efflux pumps (*tetK*, *tetL*), consistent with environmental persistence and potential horizontal gene acquisition. Our study underscores the potential of *B. mobilis* and *C. campinensis* in bioremediation strategies for heavy metal-contaminated soils. Additionally, the co-selection of resistance to both $Cd^{2+}$and antibiotics highlights the ecological complexity of contaminated environments. Future work should explore the molecular pathways driving these adaptive traits and extend susceptibility testing protocols to better assess bacterial responses under prolonged environmental and antibiotic stress.

KEYWORDS

Bacillus **mobilis, Cupriavidus campinensis, cadmium remediation, antibiotic susceptibilitytesting, growth dynamics, carbon metabolism, environmental pollution**

Introduction

Cadmium (Cd^{2+}) is one of the most toxic nonessential heavy metals and its contamination poses significant risks to human health and ecosystems. Chronic exposure to Cd^{2+}can lead to severe health issues in humans, including kidney damage, bone fractures, and cancers (Jarup et al., 1998; Waalkes, 2000). Due to its classification as persistent, bioaccumulative, and toxic, Cd^{2+} has been identified as one of the 31 Priority Chemicals for action under the U.S. Environmental Protection Agency's (EPA) National Partnership for Environmental Priorities (US EPA, 2024). Together with lead and mercury, Cd^{2+} is one of only three heavy metals designated by the U.S. Environmental Protection Agency as priority hazardous air pollutants for which emissions must be eliminated or considerably reduced in industrial processes such as coal- and oil-fired power generation (US EPA, 2024). In ecosystems, Cd^{2+}disrupts soil microbial activity and plant growth, reducing agricultural productivity and biodiversity (McLaughlin and Singh, 1999). Current policies aim to limit Cd^{2+}emissions through regulations on industrial discharges and the use of Cd^{2+}-containing fertilizers (United Nations Environment Programme, 2010). Despite these efforts, continuous monitoring and stricter enforcement of regulations are necessary to protect human health and the environment from Cd^{2+}exposure.

Techniques for the removal and immobilization of heavy metals in contaminated soils have included physical, chemical, and biological methods, as well as a mixture of multiple methods (Lee et al., 2009; Sánchez-Castro et al., 2023). Physical methods include encapsulation (Pandey et al., 2012) and electrokinetic removal (Hawal et al., 2023); however, encapsulation only contains the contaminants in the soil (Liu et al., 2018) and electrokinetic removal is expensive and difficult to implement on a large scale (Sun et al., 2023). Chemical processes include stabilization (Lee et al., 2009), but changes in soil pH could decrease the effectiveness of the treatment since the metal is not removed (Lombi et al., 2003). Soil properties such as pH and organic matter content play crucial roles in Cd^{2+}mobility and bioavailability (Kabata-Pendias, 2010). A combination of biological methods including phytoremediation and bio-augmentation poses a green method of removal and are being promoted to mitigate Cd^{2+}contamination and restore soil health (Salt et al., 1995; Clemens, 2006; Simmer and Schnoor, 2022). For instance, species of cadmium-resistant microbes have been shown to have high removal efficiencies and increase seed germination and growth rates of plants (Lata et al., 2021; Arce-Inga et al., 2022). For heavy metal alleviation, a sustainable alternative to mitigate Cd^{2+}soil toxicity includes the use of beneficial microbes with heavy metal removal abilities. Cadmium-tolerant bacteria (CdtB) such as *Enterobacter* sp., *Bacillus* sp., sulfate-reducing bacteria, and plant growth-promoting rhizobacteria (Arce-Inga et al., 2022; Bravo and Braissant, 2022) have received more attention in recent years. Future research should focus on enhancing the efficiency of remediation techniques and developing sustainable agricultural practices to prevent Cd^{2+}accumulation in soils. Moreover, it is important to identify diverse CdtB for use in green and cost-effective remediation of contaminated soils. Indeed, the application of metal-resistant bacteria in bioremediation presents promising opportunities for wastewater treatment, the restoration of contaminated soils, and bioprecipitation (Diels et al., 1995; Sreedevi et al., 2022; Nnaji et al., 2024; Abbas et al., 2025; Qattan, 2025).

Bacteria exposed to heavy metals like Cd^{2+}often develop resistance through similar genetic pathways used for antibiotic resistance, including efflux pumps and resistance genes (Seiler and Berendonk, 2012; Bravo and Braissant, 2022). These shared mechanisms can lead to the co-selection of CdtB and antibiotic-resistant bacteria in environments contaminated with heavy metals (Baker-Austin et al., 2006). Studies have shown that CdtB strains frequently exhibit resistance to multiple antibiotics, indicating a co-selection between metal resistance and multidrug resistance (Stepanauskas et al., 2006). Furthermore, horizontal gene transfer facilitated by mobile genetic elements such as plasmids can disseminate both metal-resistance and antibiotic-resistance genes among bacterial populations (Baker-Austin et al., 2006; Seiler and Berendonk, 2012). This relationship between metal and antibiotic resistance underscores the need for integrated management strategies addressing pollutants. Effective regulation of heavy metal emissions and prudent use of antibiotics are crucial to mitigating the spread of resistant bacterial strains in the environment.

The microbial metal reduction reaction is energy-dependent, and detoxifying bacteria such as CdtB require nutrients that may be limited in soils depleted of organic matter (Wagner-Döbler, 2003). Soil properties, particularly carbon and nutrient availability, and pH, significantly influence the success of bacterial reduction and subsequent volatilization and immobilization during bioremediation (Wagner-Döbler, 2003; Cattani et al., 2009). It has been reported that organic matter addition significantly increased As, Hg and Cd volatilization and immobilization from investigated soils (Yang et al., 2007; Huang et al., 2012; Liu et al., 2019). Also, adding phosphorus compounds to manage Cd^{2+} and Pb^{2+}-contaminated soils provides microorganisms with an essential nutrient, thereby enhancing microbial activity in these soils (Park et al., 2011). Given that microbial metal reduction can be utilized to remove heavy metals from contaminated soils by bio-augmentation and nutrient supplementation, it is essential to identify nutrients such as carbon substrates that enhance microbial growth when cultured in the laboratory.

The average concentration of Cd^{2+} in uncontaminated soil worldwide is 0.36 mg/kg, but it can range from 0.01 to 1 mg/kg (Kubier et al., 2019). Depending on the type of pollution, soil Cd^{2+} concentrations can be up to 344 mg/kg (by leaching of solid waste) and 74 mg/kg (by atmospheric deposition) in contaminated soils (Voglar and Lestan, 2010; Bi et al., 2006). In this study, we characterized bacterial strains isolated from Cd^{2+} spiked soil (2,043 mg/kg) of about one order of magnitude compared to average prevailing concentration levels in highly contaminated soils yielding CdtB species. Given the reported higher frequencies of antibiotic resistance in bacteria within metal-contaminated ecosystems (McArthur and Tuckfield, 2000; Stepanauskas et al., 2006) it is crucial to monitor the selection for antibiotic resistance in bacteria with bioremediation potential, as this has significant implications for human health. Forsberg et al. (2012) found evidence of the lateral transfer of multidrug-resistant genes from soil bacteria to human pathogens, highlighting the importance of monitoring antibiotic-resistance in bacteria.

Antibiotic susceptibility testing has been done routinely using several methods such as the measurement of inhibition zones in agar diffusion tests (e.g., Kirby-Bauer), turbidity-based measurements, and the counting of colony-forming units after serial dilution (Jorgensen and Ferraro, 2009) or determination of the minimal

inhibitory concentration (MIC) in serial dilutions as recommended by the Clinical and Laboratory Standards Institute (Clinical and Laboratory Standards Institute [CLSI], 2023). These conventional methods rely on static acquisition of single data points or regular-interval growth determinations (off-line susceptibility testing) and overlook the antibiotic-specific dynamic growth profiles of target microorganisms. Theophel et al. (2014) demonstrated that different microorganisms exhibit varying susceptibility to different antibiotics at different growth stages and times. In this study, we utilized on-line analysis of antibiotic susceptibility testing to provide robust information about CdtB growth kinetics with high temporal resolution in the presence of varying antibiotic concentrations in 96-well Sensititre microplates. Moreover, the on-line susceptibility analysis integrates simultaneous cultivation and assessment of antibiotic impact on bacterial growth dynamics. By combining these approaches with carbon substrate utilization profiles (BIOLOG® EcoPlate), a better understanding of CdtB growth kinetics and metabolic potential could be achieved.

The primary objectives of this study were to identify and characterize CdtB species inhabiting elevated Cd^{2+}amended soil, as well as to evaluate their antibiotic resistance and carbon utilization profiles, in order to enhance the efficiency of Cd^{2+}remediation in contaminated soils. In addition, we aimed at using the Comprehensive Antibiotic Resistance Database Resistance Gene Identifier (CARD-RGI) tool and Python applications to predict the antibiotic resistance genes (ARG) in isolated CdtB species. The findings of this study hold significant implications for the use of novel microorganisms in immobilization or detoxification of Cd^{2+}in polluted soils and for the potential augmentation of the remediation process through biostimulation with optimal carbon substrates.

Materials and methods

Isolation and identification of CdtB species from elevated cadmium amended soil

Two 50g soil samples collected from a temperate forest (Greencastle, IN) were incubated for 2 weeks at room temperature with and without Cd^{2+}amendment. The amended soil received 2 mL of 19.5 mM Cd^{2+}solution [6g of $Cd(NO_3)_2.4H_2O$/L (Mallinckrodt, St. Louis, USA)] to establish a high Cd^{2+}stress comparable to cadmium concentrations reported in zinc sulfide ore and smelting dust (430–1500 mg kg^{-1}; Bi et al., 2006), thereby simulating an ecologically relevant high-stress environment representative of metal-contaminated sites. After incubation, we vortexed 2 g of control and Cd^{2+}-amended soils in 18 mL of Remel TM Butterfield's Phosphate Buffer (Hardy Diagnostics, California, USA). The resulting suspension was diluted at 10^{-3} and 100 μL of this latter was inoculated on Peptone Yeast Cd^{2+}-amended agar plates in duplicate. Culture media used to select for Cd^{2+} resistant bacterial growth were as follows: Peptone Yeast (PY) medium consisted of 5 g peptone, 3 g yeast extract, and 15 g/L agar powder maintaining pH 7. 10 mL of 1.0M $CaCl_2$ was added to make the solution 10 mM $CaCl_2$, and amended with 1 mL of 6g of $Cd(NO_3)_2{\cdot}4H_2O$/L to make the medium select for Cd^{2+}resistant microbes. All plates were incubated aerobically at 37 C for 48 h. Culturable Cd isolates used in this study were identified by colony PCR followed by 16S rRNA gene sequencing. Purified PCR products were submitted for sequencing to Genewiz Inc. (South Plainfield, NJ, USA). For colony PCR, single colonies from nutrient agar plates were screened using OneTaq 2X Master Mix with Standard Buffer (New England Biolabs, Ipswich, MA; Cat. No. M0482), following the manufacturer's instructions. Each 50 µL PCR reaction contained 25 µL OneTaq 2X Master Mix, 1 µL of 10 µM forward primer, 1 µL of 10 µM reverse primer, 22 µL ultrapure H_2O, and 1 µL of cell suspension as the DNA template. Thermocycling conditions were: initial denaturation at 94 C for 2 min; 35 cycles of 94 C for 30 s, 57 C for 30 s, and 68 C for 2 min; and a final extension at 68 C for 5 min, followed by a 4 C hold.

The control and spiked soils were oven-dried at 35 C and grounded for metal analysis to assess the concentrations (ppm) of heavy metals in the soil samples. X-ray fluorescence (XRF) analysis was conducted on each soil sample using a Bruker Tracer 5 g handheld XRF unit fitted with a rhodium (Rh) source, a graphene window silicon drift detector (SDD), and an 8 mm collimator as described in Akinwole et al. (2024).

Evaluation of antibiotic resistance of CdtB colonies by using Sensititre™ GN4F and GPALL1F microplates

The Sensititre method for testing antibiotic susceptibility was performed according to the manufacturer's instructions. Sensititre Gram-Positive GPALL1F (Thermo Scientific, USA) plate was used for *Bacillus mobilis* (Liu et al., 2017), while Sensititre Gram-Negative GN4F (Thermo Scientific, USA) plate was used for *Cupriavidus campinensis* (Goris et al., 2001). In brief, a pure culture of the CdtB isolate, which had been grown for 48 h on nutrient agar, was used with sterile water to make a 0.5 McFarland turbidity suspension. The Sensititre plate GN4F consisted of serial 2-fold dilutions of 24 antimicrobials and the Sensititre plate GPALL1F consisted of serial 2-fold dilutions of 23 antimicrobials (Supplementary Table S1).

From the bacterial suspension, 20 µL was transferred into a 5.5 mL Muller Hinton broth tube, and then 50 µL was transferred into each well of the GN4F and GPALL1F plate using an 8-channel pipette. The plate was covered with an adhesive seal provided with the kit and incubated on a SPECTROstar Nano (BMG LABTECH) plate reader for automated reading for 72 h at 35 C. During incubation, orbital shaking conditions were selected (4 mm amplitude and 30 s shaking cycles), and measurements were taken every 25 min at a wavelength of 660 nm. Growth analysis was accompanied by controls cultured in the absence of antibiotics to obtain reference curves and sterile media controls without antibiotics for quality control testing.

Evaluation of metabolic profiles of Cd-resistant colonies by BIOLOG™ Ecoplates

Each isolate was cultured in nutrient agar broth at 37 °C for 48h and 150 µL of 1:1000 dilution of each isolate was pipetted into BIOLOG Ecoplate (BIOLOG Inc., Hayward, CA). Ecoplates were incubated aerobically at room temperature for 7 days to assess metabolic profile analysis. The rate of utilization was indicated by

TABLE 1 (a) Heavy metal analysis showing soil concentration means (±2SE; n = 5), and (b) blastn results, according to the NCBI database.

a) Soil type	Cd (ppm)	Pb (ppm)	Cu (ppm)	Zn (ppm)	Cr (ppm)
Control soil	<LOD*	22 ± 11	16 ± 6	80 ± 6	80 ± 15
Cadmium-spiked soil	2043 ± 43	20 ± 6	18 ± 7	78 ± 7	73 ± 25
b) Strain Description	**Accession No**	**Max Identity (%)**	**Max score**	**Total score**	**Notes**
Bacillus mobilis strain MCCC 1A05942	NR_157731.1	100	2787	2787	Within the *B. cereus* group (Liu et al., 2017)
Cupriavidus campinensis strain WS2	NR_025137.1	100	2741	2741	Formerly known as *Ralstonia campinensis* (Goris et al., 2001)

* below level of detection.

the reduction of the tetrazolium salt (a redox indicator dye) that changes from colorless into purple in the Ecoplate wells. The color development was monitored every 24 h as optical density (OD) with SPECTROstar Nano (BMG LABTECH) microplate reader at a wavelength of 590 nm. The OD values of Ecoplate at 120 h were used to analyze bacterial carbon source utilization since these represented the optimal range of OD readings in our study in the absence of fungal growth biases (Zhang et al., 2013). The metabolic profile of each isolate was calculated according to the average well color development (AWCD) defined as the arithmetic average of the absorbance values for each substrate (Harch et al., 1997), AWCD indicates the total metabolic capacity of each bacterial species in terms of carbon-source utilization. The five carbon substrate guilds proposed by Weber and Legge (2009) were utilized: 1) carbohydrates, 2) carboxylic and acetic acids, 3) amino acids, 4) polymers, and 5) amines and amides. For each guild, the blank-corrected absorbance values of the substrates at 120 h were summarized and expressed as a percentage of the total absorbance value of the plate (Weber and Legge, 2009).

Data visualization and statistics of the comprehensive antibiotic resistance database (CARD) antibiotic resistance ontology (ARO) of isolates

ARGs were identified *in silico* from the genome assemblies corresponding to our isolates (*B. mobilis*, GCA_001884045.1; *C. campinensis*, GCF_042653745.1). Isolate identity was confirmed via partial 16S rRNA sequencing and BLAST analysis, which showed 100% identity to *B. mobilis* strain MCCC 1A05942 (NR_157731.1) and *C. campinensis* strain WS2 (NR_025137.1) (Liu et al., 2017; Goris et al., 2001). ARGs were detected using the CARD Resistance Gene Identifier (CARD-RGI; Alcock et al., 2023) and custom Python scripts. In this study Matplotlib (version 3.9.4) and Seaborn (version 0.13.2) Python libraries widely used for data visualization were used to generate sunburst classification plots based on the CARD antibiotic resistance ontology, helping to visually represent the hierarchical structure and distribution of potential resistance genes present in *B. mobilis* and *C. campinensis*. Matplotlib is a core plotting library that works with NumPy (version 2.0.2) and provides an object-oriented application programming interface for embedding plots into applications. It supports various graphical user interface toolkits such as Tkinter, wxPython, Qt, and GTK. Seaborn builds on Matplotlib and integrates seamlessly with pandas (version 2.3.0). It offers a high-level, declarative interface for creating statistical graphics, making it easier to translate complex data into clear visual insights (Bisong, 2019).

Data analysis

The values in the figures and tables correspond to the average of triplicate data ±standard error (SE) for both antibiotic susceptibility testing and carbon substrate utilization data. For the carbon substrate utilization data, the AWCD index was calculated with the formula:

$$AWCD = \Sigma (C\,i - R)/n,$$

where Ci is the absorbance of the carbon source, R is the absorbance of the control well, and n is the number of carbon substrates (31 for EcoPlates). When Ci–R < 0, the values were set to 0 to minimize bias. Assessing the utilization profiles involves grouping the 31 carbon sources into five guilds according to Weber and Legge (2009) and evaluating changes in the percent guild utilizations over the study period. This method effectively reduces the 31-dimensional space of each plate into five dimensions, facilitating easier plotting and interpretation. In addition, the growth dynamic of cells exposed to carbon substrate reaching an OD > 1.8 at the end of the incubation period is termed high utilization, growth dynamic at OD < 1.8 but >0.2 is termed medium utilization and OD ≤ 0.2 is inhibitory.

Resistance analysis was performed using CARD-RGI with Perfect, Strict, and Loose detection paradigms. Perfect hits indicate >95% identity and coverage to known resistance genes. Strict hits show >40% identity with coverage criteria. Loose hits represent <40% identity but maintain biological relevance. Statistical analysis and visualization were performed using Python with matplotlib and seaborn libraries.

Results

Strain identification and morphology characterization

To provide a quantitative assessment of heavy metals present in both control and amended soils, the results of bulk soil XRF analysis conducted on each soil sample are shown in Table 1a. There were no

significant differences in spiked and control soils for major heavy metals (Pb, Cu, Cr, and Zn) in this region, however, Cd^{2+}spiked soil showed an extreme increase in the concentration of 2,043 ± 43 ppm compared to below the level of detection in the control soil. This demonstrated that the spiked soil was adequately amended as a cadmium-elevated soil environment.

A total of six culturable bacteria exhibiting distinct colony characteristics such as opacity, texture, form, size, and margin surface were identified, however, the two most metabolic active on Biolog Ecoplate were selected for further biochemical and molecular characterizations. For the two colonies selected, a BLAST search of the commercially determined sequences against publicly available sequences in the NCBI database indicated 100% identity to *B. mobilis strain MCCC 1A05942* (accession no. NR_157731.1) and 100% to *C. campinensis* strain WS2 (accession no. NR_025137.1) (Table 1b) formerly known as *Ralstonia campinensis* (Liu et al., 2017; Goris et al., 2001). *B. mobilis* produces milky-white, circular, opaque colonies measuring 2–3 mm in diameter after 48 h of incubation at 32 °C on LB medium (Liu et al., 2017). In contrast, *C. campinensis* forms small, round colonies (sometimes with slightly scalloped margins) that are smooth, convex, and transparent, with an average diameter of ~0.5 mm after 24 h of incubation on TSA at 30 C (Goris et al., 2001).

Effects of various antibiotics on B. mobilis and C. campinensis growth dynamics

To examine the dynamic effects of antibiotics over time, we implemented a method that integrates simultaneous cultivation and assessment of antibiotic impact on bacterial growth through automated OD measurements taken at 25-min intervals. This approach revealed varying effective exposure times and concentration-dependent effects on the growth dynamics of *B. mobilis* and *C. campinensis* isolated from cadmium-amended soil.

In the Sensititre Gram-Negative GN4F plate for *C. campinensis,* after a lag phase of approximately 10 h, the control culture (without antibiotics) exhibited a sharp increase in OD until about the 24-h mark, followed by a gradual decrease and plateau for the remainder of the incubation period (Figures 1, 2). Compared with the antibiotic-free control, *C. campinensis* cells exposed to imipenem, tigecycline, levofloxacin, ceftriaxone (Figure 1) and 10 more antibiotics (Table 2) were unable to grow (i.e., inhibited) at any concentrations. However, in the case of ceftriaxone, after a prolonged lag phase up to 50 h, growth comparable to that of the antibiotic-free control was observed at the lowest concentration of 0.5 μg mL^{-1} (Figure 1d).

Figure 2 displayed various growth dynamics and concentration-dependent effects in the case of six antibiotics. Cells exposed to different concentrations of nitrofurantoin, ertapenem (Figures 2a,b), and cefazolin (Table 2) had similar growth patterns with antibiotic-free control; however, the final OD values did not reach that of the control culture. Despite a lag phase of >24 h, cells exposed to 8/2, 16/2, and 32/2 μg mL^{-1} of ticarcillin/clavulanic acid constant two began to grow slightly below antibiotic-free control. At 64/2 μg mL^{-1} inhibitory effects of ticarcillin/clavulanic acid, constant two was seen on the growth of *C. campinensis* (Figure 2c). Extended lag phases (approximately 36 h) were observed in cultures containing beta-lactam class; piperacillin (Figure 2d) and ampicillin (Table 2) at all concentrations and began to grow exponentially at a rate slightly below that of the antibiotic-free control. More complex concentration-dependent effects were observed in the case of doripenem, aztreonam (Figures 2e,f) and meropenem (Table 2). 4 μg mL^{-1} of doripenem was inhibitory on cells for the entire incubation period while after an extended lag phase of 36 h at a concentration of 2 μg mL^{-1} cells began to grow and plateau approximately at 52 h for the remainder of the incubation period. Cells exposed to 0.5 and 1 μg mL^{-1} showed a similar pattern to the control with a lag phase of 10 h, a sharp increase in OD until 24 h, and a gradual decrease/plateau for the remainder of the incubation period (Figure 2e). The lag phase was similar to the control culture at all concentrations for aztreonam, however, after 8 h exponential growth, cells exposed to 16 μg mL^{-1} of aztreonam plummeted and did not show bacterial growth for the remainder of the incubation period (Figure 2f). After a lag phase of 12 h, cells exposed to 1, 2, 4 and 8 μg mL^{-1} of aztreonam began to grow and decline gradually at 24 h for the remainder of the incubation period.

With a similar pattern of cells' growth dynamics in Ertapenem's (Figure 2b), cells exposed to meropenem were resistant at low concentrations (0.5, 1, and 2 μg mL^{-1}), but growth curves at concentrations of four and 8 μg mL^{-1} exhibited extended lag phases (approximately 32 h), accompanied by a slight increase in growth with lower OD values but not significantly different from samples with 0.5, one and 2 μg mL^{-1}. Growth curves at all concentrations were at a rate slightly below that of the antibiotic-free control (Table 2).

Ceftazidime concentrations of 4 μg mL^{-1} and above were inhibitory on cells for the entire incubation period (Table 2). Cells in 2 μg mL^{-1} exhibited extended lag phase up to approximately 36 h, accompanied by a shallower growth curve slope and lower OD values than control cells. For cells exposed to 1 μg mL^{-1}, after a lag phase of approximately 10 h as the control culture, exhibited a gradual increase in OD until about the 48-h mark, followed by a gradual decrease and plateau for the remainder of the incubation period.

In the Sensititre Gram-Positive GPALL1F plate for B. *mobilis,* after a lag phase of approximately 6 h, the control culture without antibiotics exhibited a sharp increase in OD until about the 15-h mark, followed by a plateau for the remainder of the incubation period (Figures 3, 4). Approximately 50% of (a total of ten) antibiotics showed limited activity against *B. mobilis,* at all concentrations tested and five agents were ineffective at lower concentrations (Table 2). Representative growth dynamics of cells exposed to different concentrations of erythromycin, ampicillin, clindamycin, and vancomycin (Figure 3) had identical growth patterns similar to antibiotic-free control; however, with a slightly extended lag phase of about 12 h. Generally, growth curves at lower concentrations were not significantly different from that of the antibiotic-free control while curves at higher concentrations showed more deviation from controls. Other similar antibiotics that did not inhibit the growth of *B. mobilis* are shown in Table 2.

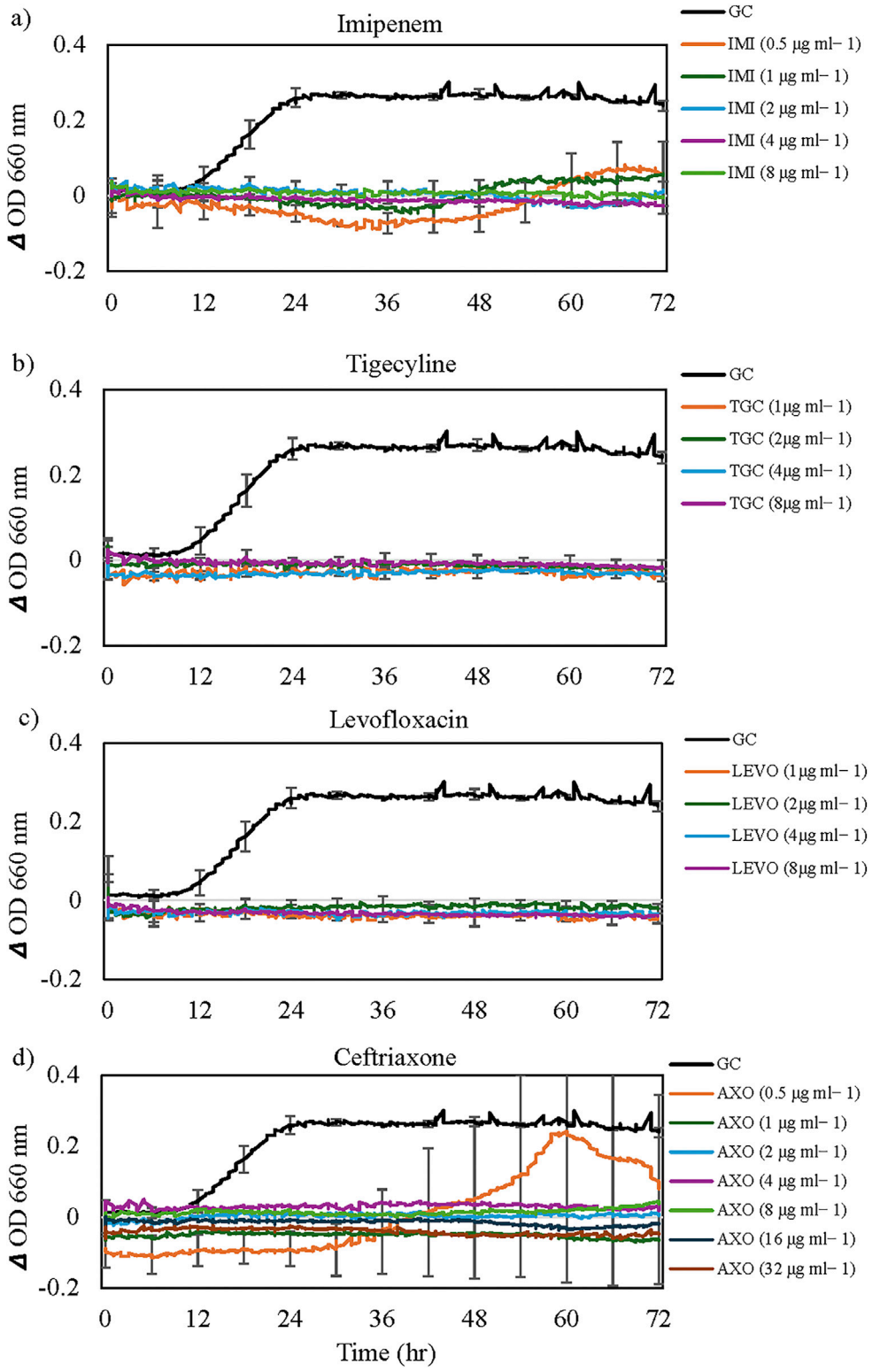

FIGURE 1
Inhibitory effects of antibiotics tested on the growth of *Cupriavidus campinensis*. Results for only **(a)** imipenem, **(b)** tigecycline, **(c)** levofloxacin and **(d)** ceftriaxone are shown, but inhibitory effects with similar patterns (except for Ceftriaxone) were observed for 15 out of 24 antibiotics tested (Table 2). For visual clarity, standard error bars (n = 3) are only presented for selected time points every 6 h. GC = Growth Control. Note the extended lag phase and partial growth promotion at low concentration (0.5 µg mL^{-1}) for Ceftriaxone.

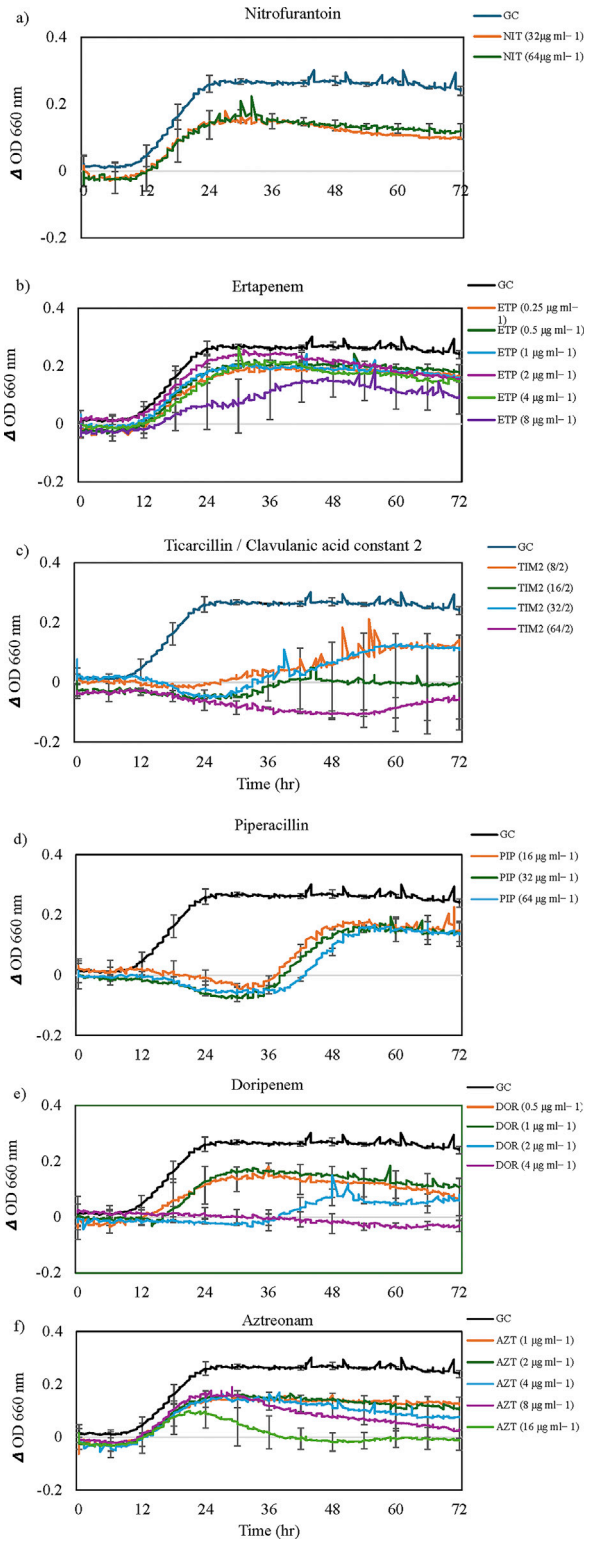

FIGURE 2
The growth dynamics of *Cupriavidus campinensis* in the presence of selected antibiotics **(a-f)**. Each data point (time resolution over 72 h) represents mean values of triplicate cultivations, normalized with data from identical incubations without bacterial cells (sterile controls). Using a time resolution of 25 min, each curve represents 576 single data points. For visual clarity, standard errors bars (n = 3) are only presented for selected time points every 6 h. GC = Growth Control. Note the extended lag phase for some antibiotics (e.g., piperacillin and ampicillin) and partial growth promotion at low concentrations for some antibiotics.

TABLE 2 Sensitivity of *Bacillus mobilis* and *Cupriavidus campinensis* to various antibiotics and their cellular targets. Susceptible (S), Resistance (R), potential categorization (PC) is based on MIC ($\mu g\ mL^{-1}$).

C. Campinensis			
Antibiotic	Antibiotic's cellular targets	S Or R based on MIC ($\mu g\ mL^{-1}$) at <36h	PC based on MIC ($\mu g\ mL^{-1}$) at >36h
Amikacin, Tigecycline Tetracycline, Minocycline, Gentamicin, Tobramycin	30S ribosomal subunit (inhibits protein synthesis)	S	S
Piperacillin/Tazobactam constant 4	Penicillin-binding proteins (PBPs) (Piperacillin inhibits cell wall synthesis, Tazobactam is a beta-lactamase inhibitor)	S	S
Ticarcillin/Clavulanic acid constant 2	PBPs (Ticarcillin inhibits cell wall synthesis, Clavulanic acid is a beta-lactamase inhibitor)	R at MIC ≥64/2, S	R at MIC ≥64/2, S
Levofloxacin, Ciprofloxacin	DNA gyrase and topoisomerase IV (inhibits DNA replication)	S	S
Nitrofurantoin	Multiple targets, including ribosomal proteins and DNA (inhibits bacterial growth)	R	R
Doripenem	PBPs (inhibits cell wall synthesis)	R at MIC ≥2, S	at MIC = 2, R at MIC ≥4, S
Ertapenem, Meropenem Cefazolin	PBPs (inhibits cell wall synthesis)	R	R
Trimethoprim/Sulfamethoxazole	Dihydrofolate reductase (Trimethoprim) and dihydropteroate synthase (Sulfamethoxazole) (inhibit folic acid synthesis)	S	S
Imipenem Cefepime	PBPs (inhibits cell wall synthesis)	S	S
Piperacillin Ampicillin	PBPs (inhibits cell wall synthesis)	S	R
Ceftazidime	PBPs (inhibits cell wall synthesis)	R at MIC ≥4, S	R at MIC ≥4, S
Ampicillin/Sulbactam 2:1 ratio	PBPs (Ampicillin inhibits cell wall synthesis, Sulbactam is a beta-lactamase inhibitor)	S	S
Aztreonam	PBPs (inhibits cell wall synthesis)	R	at MIC ≥16, S
Ceftriaxone	PBPs (inhibits cell wall synthesis)	S	at MIC ≤0.5, R
B. mobilis			
Antibiotic	Antibiotic's cellular targets	S Or R based on MIC ($\mu g\ mL^{-1}$) at <36h	PC based on MIC ($\mu g\ mL^{-1}$) at >36h
Chloramphenicol	50S ribosomal subunit (inhibits protein synthesis)	S	at MIC ≤4, R
Daptomycin	Cell membrane (causes depolarization and cell death)	R	R
Gentamicin	30S ribosomal subunit (inhibits protein synthesis)	S	at MIC ≤4, R

(Continued on following page)

10.3389/fenvs.2025.1668462

TABLE 2 (*Continued*) Sensitivity of *Bacillus mobilis* and *Cupriavidus campinensis* to various antibiotics and their cellular targets. Susceptible (S), Resistance (R), potential categorization (PC) is based on MIC ($\mu g\ mL^{-1}$).

B. mobilis			
Antibiotic	Antibiotic's cellular targets	S Or R based on MIC ($\mu g\ mL^{-1}$) at <36h	PC based on MIC ($\mu g\ mL^{-1}$) at >36h
Rifampin	RNA polymerase (inhibits RNA synthesis)	R	R
Trimethoprim/Sulfamethoxazole	Inhibits dihydrofolate reductase (Trimethoprim) and dihydropteroate synthase (Sulfamethoxazole) (inhibit nucleic acid and protein synthesis)	R at MIC ≥4/76, S	at MIC ≥4/76, S
Tetracycline	30S ribosomal subunit (inhibits protein synthesis)	R at MIC = 16, S	R at MIC = 16, S
Erythromycin, Clindamycin, Linezolid, Quinupristin/Dalfopristin	50S ribosomal subunit (inhibits protein synthesis)	R	R
Ampicillin, Penicillin Oxacillin +2% NaCl	PBPs (inhibits cell wall synthesis)	R	R
Vancomycin	D-Ala-D-Ala terminus of cell wall precursors (inhibits cell wall synthesis)	R	R
Levofloxacin	DNA gyrase and topoisomerase IV (inhibits DNA replication)	R at MIC ≥1, S	R at MIC ≥2, S
Tigecycline	30S ribosomal subunit (inhibits protein synthesis)	R at MIC ≥0.25, S	at MIC ≥0.25, S
Moxifloxacin	DNA gyrase and topoisomerase IV (inhibits DNA replication)	R at MIC ≥1, S	at MIC ≥2, S
Streptomycin	30S ribosomal subunit (inhibits protein synthesis)	S	S
Ciprofloxacin	DNA gyrase and topoisomerase IV (inhibits DNA replication)	S	R
Nitrofurantoin	Multiple targets, including ribosomal proteins and DNA (inhibits bacterial growth)	S	R
D Test 1 D Test 2	tests for inducible clindamycin resistance in the presence of erythromycin	R	R
Cefoxitin screen	PBPs (inhibits cell wall synthesis)	R	R

10.3389/fenvs.2025.1668462

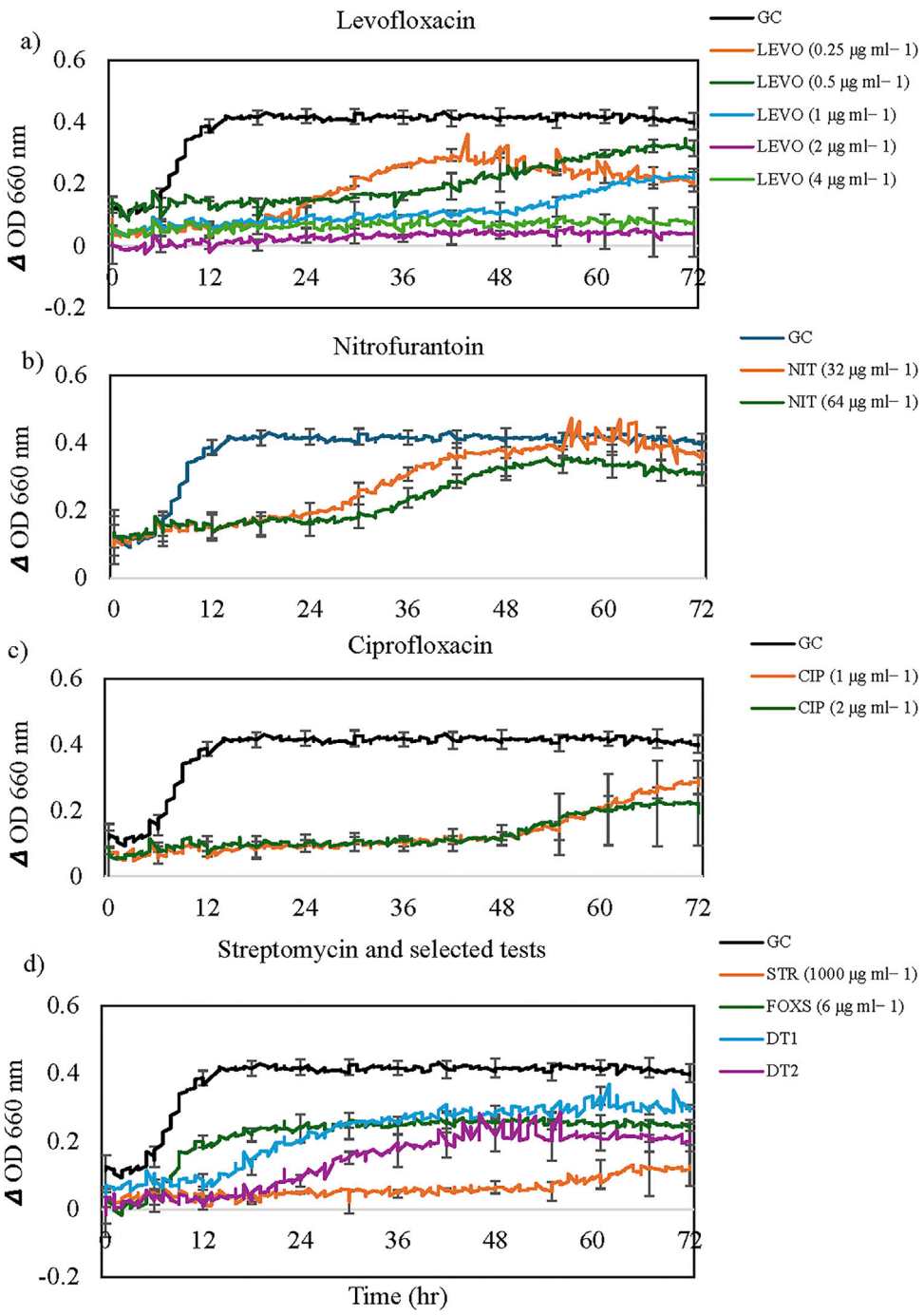

FIGURE 3
The growth dynamics of *Bacillus mobilis* in the presence of selected antibiotics: **(a)** Levofloxacin, **(b)** Nitrofurantoin, **(c)** Ciprofloxacin, and **(d)** Streptomycin and selected tests. Each data point (time resolution over 72 h) represents mean values of triplicate cultivations, normalized with data from identical incubations without bacterial cells (sterile controls). Using a time resolution of 25 min, each curve represents 576 single data points. For visual clarity, standard error bars (n = 3) are only presented for selected time points every 6 h. GC = Growth Control. Note the extended lag phase for some antibiotics (e.g., Levofloxacin and Ciprofloxacin) and partial growth promotion at high concentrations for some antibiotics.

More complex concentration-dependent effects were observed for the other 10 antibiotics, cefoxitin screen, and D Tests. Representative growth dynamics of cells exposed to different concentrations of levofloxacin, nitrofurantoin, ciprofloxacin, streptomycin and some selected screening tests are shown in Figure 4. Levofloxacin concentrations of two and 4 µg mL^{-1} were inhibitory on cells for the entire incubation period (Figure 4a). Cells in 0.25 µg mL^{-1} exhibited extended lag phase up to approximately 22 h, accompanied by an exponential growth curve and lower OD values than control cells. For cells exposed to 0.5 and 1 µg mL^{-1}, after a lag phase of approximately 36 h, exhibited a gradual increase in OD but lower values than control cells. This growth pattern is similar

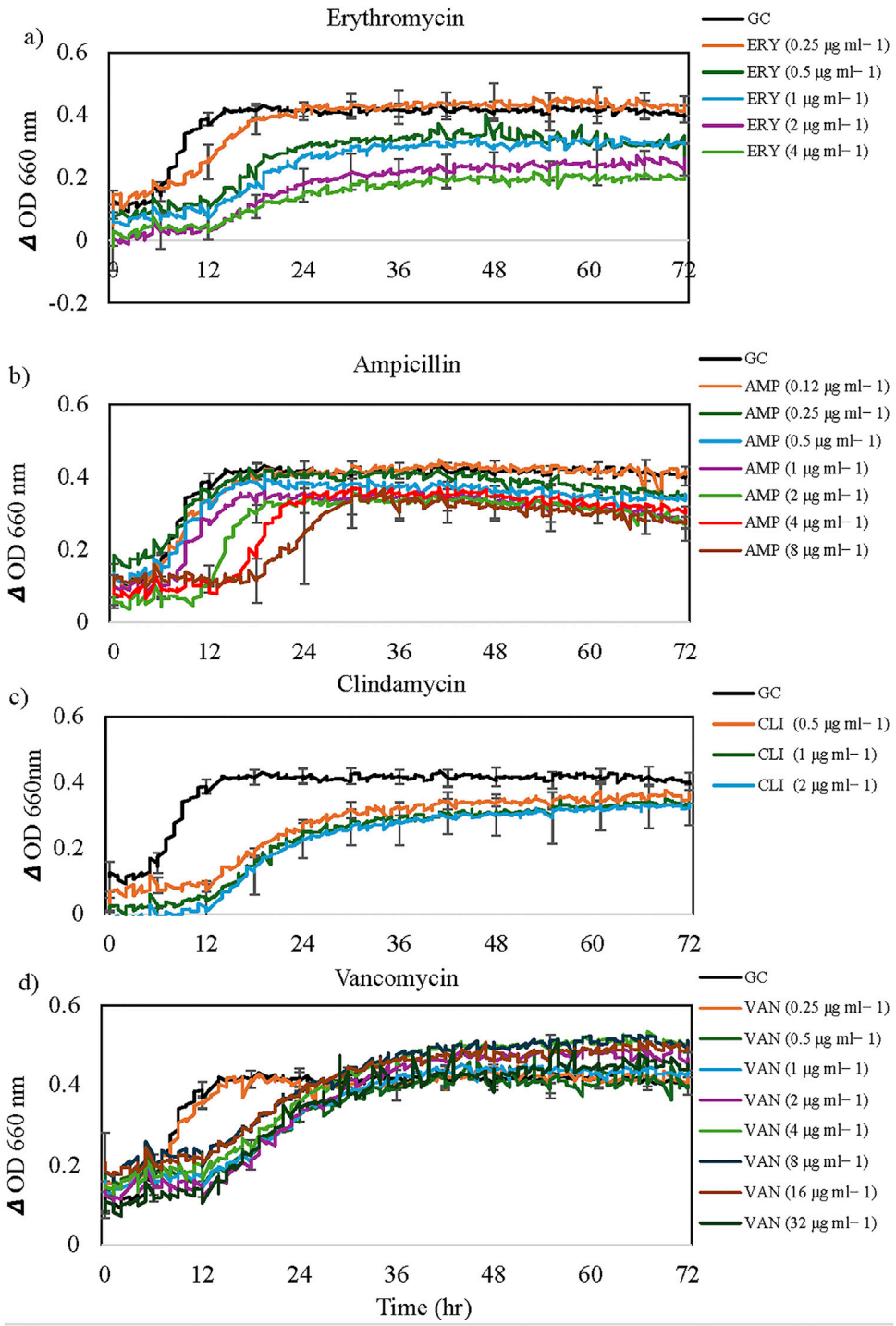

FIGURE 4
The growth dynamics of *Bacillus mobilis* in the presence of selected antibiotics: **(a)** Erythromycin, **(b)** Ampicillin, **(c)** Clindamycin and **(d)** Vancomycin. Each data point (time resolution over 72 h) represents mean values of triplicate cultivations, normalized with data from identical incubations without bacterial cells (sterile controls). Using a time resolution of 25 min, each curve represents 576 single data points. For visual clarity, standard error bars (n = 3) are only presented for selected time points every 6 h. GC = Growth Control. Note the extended lag phase for some antibiotics at higher concentrations (e.g., ampicillin).

to that observed in cells exposed to tigecycline, chloramphenicol, gentamicin, and moxifloxacin (Table 2).

Cells exposed to nitrofurantoin exhibited an extended lag phase of up to 24 h followed by exponential growth and the final OD values were not significantly different from that of the control culture (Figure 4b). In the case of ciprofloxacin, the extended lag phase reached 48h followed by a gradual increase in OD but with lower values than

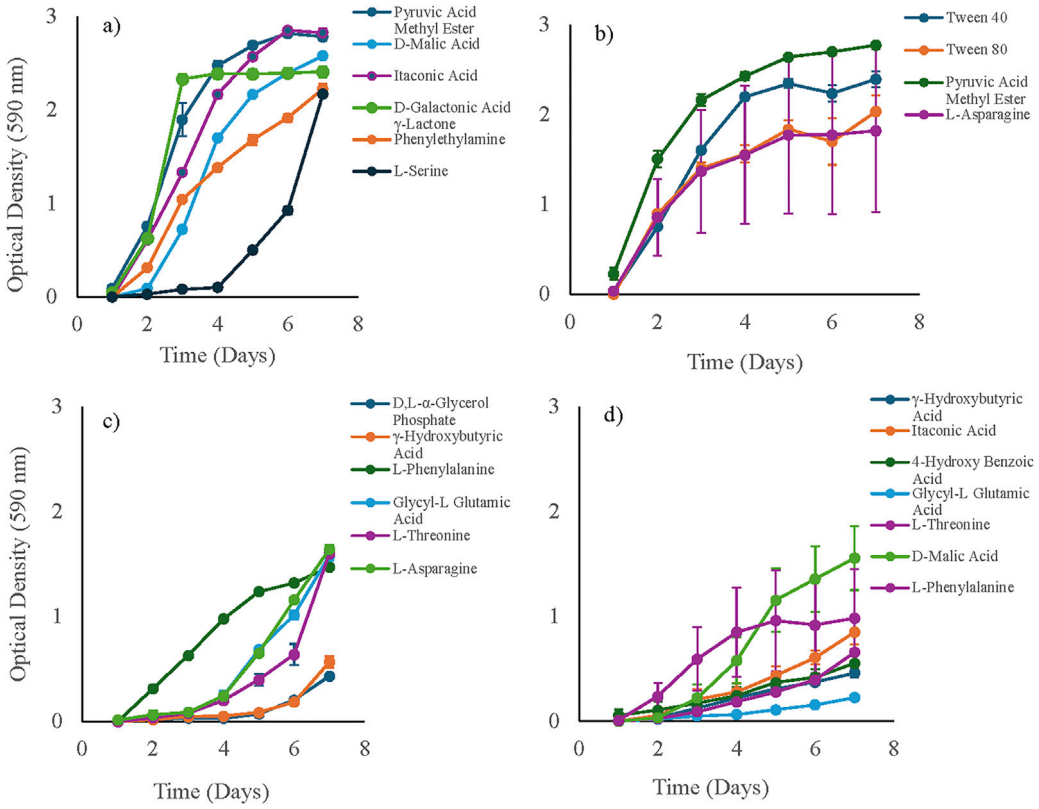

FIGURE 5
Growth dynamics of bacterial isolates exposed to 31 carbon substrates in Ecoplates, measured as OD_{590nm} over 7 days. Panels show high carbon utilization in **(a)** *Bacillus mobilis* and **(b)** *Cupriavidus campinensis* (final OD_{590} > 1.8 on day 7), and medium carbon utilization in **(c)** *B. mobilis* and **(d)** *C. campinensis* (0.2 < final OD_{590} < 1.8 on day 7). Error bars represent the standard error of the mean (n = 3).

TABLE 3 Percentage total carbon substrate utilization per guild and substrates with inhibitory effects on *B. mobillis and Cupriavidus campinensis.*

B. mobillis		*C. campinensis*	
Guild utilization (%)	Inhibitory carbon substrate within guild	Guild utilization (%)	Inhibitory carbon substrate within guild
Polymer (0.88)	Glycogen, α-Cyclodextrin **Tween 40, Tween 80**	Polymer (36.31)	Glycogen, α-Cyclodextrin
Carbohydrates (20.95)	D-Cellobiose, D-Mannitol, D-Xylose, Glucose-1-Phosphate, i-Erythritol N-Acetyl-D-Glucosamine, α-D-Lactose β-Methyl-D-Glucoside	Carbohydrates (24.19)	D-Cellobiose, D-Mannitol, D-Xylose, Glucose-1-Phosphate, i-Erythritol, N-Acetyl-D-Glucosamin α-D-Lactose, β-Methyl-D-Glucoside, **D, L-α-Glycerol Phosphate**
Carboxylic and Acetic acids (52.26)	2-Hydroxy Benzoic Acid, **4-Hydroxy Benzoic Acid**, D-Galacturonic Acid D-Glucosaminic Acid α-Ketobutyric Acid	Carboxylic and Acetic acids (13.62)	2-Hydroxy Benzoic Acid, D-Galacturonic Acid, D-Glucosaminic Acid α-Ketobutyric Acid **D-Galactonic Acid γ-Lactone**
Amino acids (14.59)	L-Arginine	Amino acids (25.74)	L-Arginine, **L-Serine**
Amine/amides (11.32)	Putrescine	Amine/amides (0.14)	Putrescine, **Phenylethylamine**

*__bold__ indicates substrates that were inhibitory in only a single isolate.

control cells (Figure 4c). Cells exposed to streptomycin (1000 μg mL^{-1}) exhibited extended lag phase up to 55 h followed by a slight increase in OD significantly lower than that of the antibiotic-free control (Figure 4d). However, Cefoxitin screen (FOXS), D test one and test two showed limited activity against *B. mobilis* (Figure 4d).

Metabolic and physiological profiles of B. mobilis and C. campinensis

In this study, we investigated the growth dynamics and metabolic profiles of *B. mobilis* and *C. campinensis* when exposed to various carbon substrates. Figure 5 indicates a broad

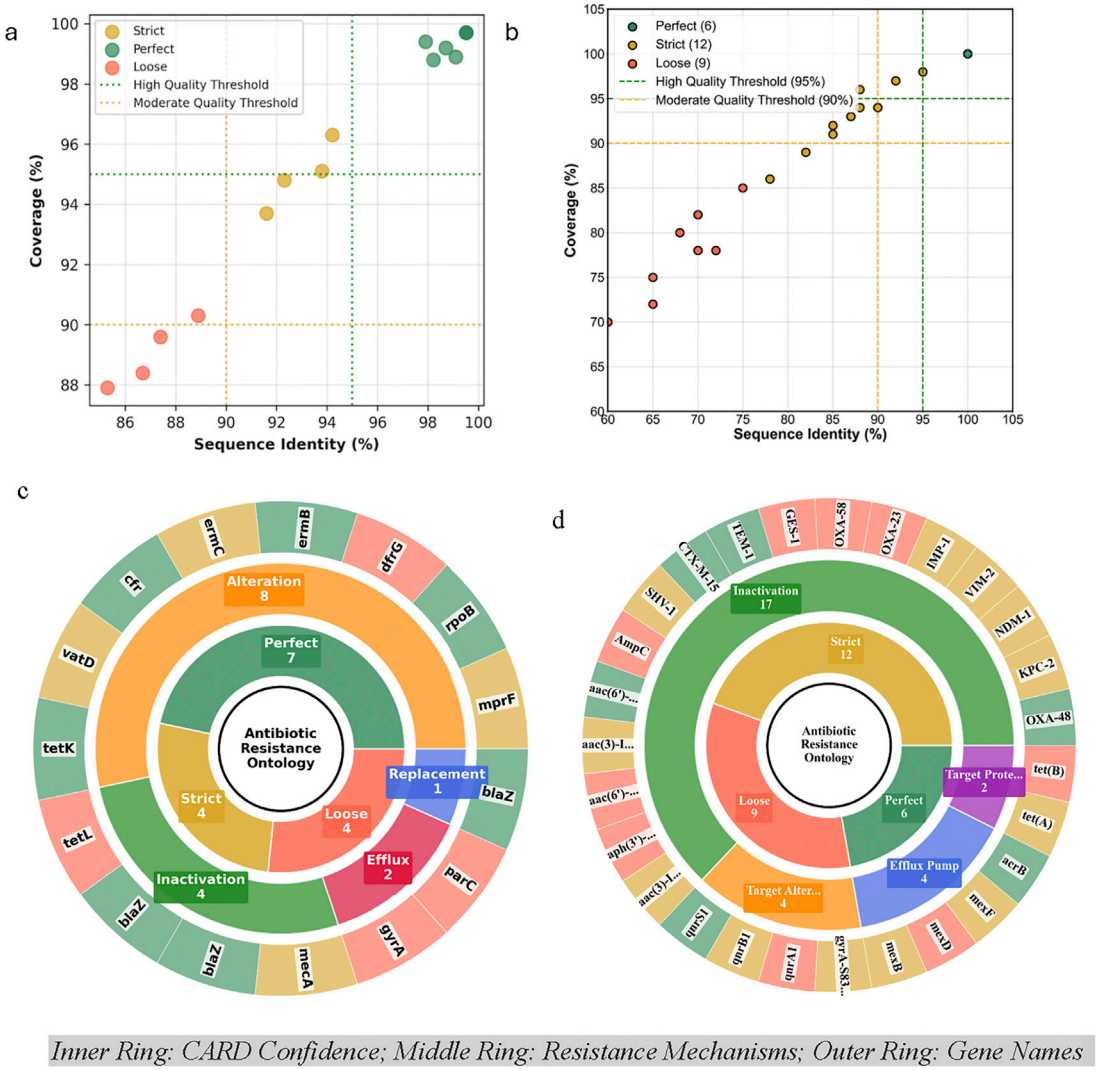

FIGURE 6
CARD Gene Annotation Quality Assessment (Identity vs Quality coverage plot) for **(a)** *Bacillus mobilis* and **(b)** *Cupriavidus campinensis*, and CARD antibiotic resistance ontology sunburst classification for **(c)** *Bacillus mobilis* and **(d)** *Cupriavidus campinensis* multi-level hierarchical gene organization which generates an annotation organized by the Perfect, Strict and Loose paradigm and resistance mechanisms. For visual clarity, aac (3)-I . . . , aac (6′). . ., aph (3′). . . are aac (3)-IIa, aac (6′)-Ib, aph (3′)-VI, respectively, while TEM-1, IMP-1, GES-1, AmpC, CTX-M-15, VIM-2, NDM-1, SHV-1, OXA-23/48/58, and KPC-2 are prefixed by bla (Supplementary Tables S1 and S2). *Target Prote/Alter = Target Protection and Target Alteration respectively.*

utilization of various carbon substrates by the bacterial isolates from cadmium-amended soil. For *B. mobilis*, the growth patterns showed significant variation depending on the carbon substrate provided. Pyruvic Acid Methyl Ester (carbohydrate), D- Malic Acid, Itaconic Acid, D-Galactonic acid γ-Lactone (carboxylic and acetic acids) and Phenylethylamine (amine/amides) exhibited the highest growth rates of *B. mobilis*, with OD values exceeding 1.8 (high utilization) over the 7 days incubation period (Figure 5a). After a lag phase of approximately 1 day, *B. mobilis* culture exhibited an exponential growth in these substrates. However, cells in L-Serine (amino acids) had an extended lag phase of 4 days before showing an increase in growth rate and reaching OD value of >1.8 on day 7. D, L-α-Glycerol Phosphate, γ-Hydroxybutyric Acid, L-Phenylalanine, Glycyl-L Glutamic Acid, L-Threonine, and L-Asparagine showed medium utilization by *B. mobilis* with OD values <1.8 but greater than 0.2 estimate for inhibitory effect (Figure 5c). Lag phase varied between 1 and 3 days for L-Phenylalanine, Glycyl-L Glutamic Acid, L-Threonine, and L-Asparagine. However, *B. mobilis* exhibited an extended lag phase of 5 days in D, L-α-Glycerol Phosphate and γ-Hydroxybutyric Acid before reaching 0.4 ± 0.02 and 0.6 ± 0.05 OD values respectively.

For *C. campinensis*, the growth dynamics also varied significantly with different carbon substrates. Tween 40, Tween 80 (polymers), L-Asparagine (amino acid) and Pyruvic Acid Methyl Ester (carbohydrate) supported the highest growth, reaching an OD value of over 1.8 (high utilization) by the seventh day (Figure 5b). *C. campinensis* exhibited medium utilization of γ-Hydroxybutyric Acid, Itaconic Acid, 4-HydroxyBenzoic Acid, Glycyl-L Glutamic

Acid, L-Threonine, D-Malic Acid and L-Phenylalanine with maximum OD between 0.2 and 1.8. However, cells in Glycyl-L Glutamic Acid exhibited reduced growth and only reached 0.22 ± 0.01 on day 7 (Figure 5d).

Inhibitory effects (OD < 0.2) were observed for both isolates when exposed to specific carbon substrates that accounts for about 65% of total carbon substrates in Ecoplates. *B. mobilis* exhibited inhibited growth in Glycogen, Tween 40, Tween 80, α-Cyclodextrin (polymers), L-Arginine (amino acid), Putrescine (amine/amides), several carbohydrates, and carboxylic and acetic acids (Table 3). Similarly, *C. campinensis* showed minimal or no growth response to Glycogen and α-Cyclodextrin (polymers), L-Arginine and L-Serine (amino acids), Putrescine and Phenylethylamine (Amine/amides) several carbohydrates, and carboxylic and acetic acids (Table 3).

The overall percent utilization of different carbon substrates grouped by guilds by both isolates highlighted their metabolic preferences. *C. campinensis* metabolized polymers and amino acids at 36.31% and 25.74% respectively compared to *B. mobilis,* with polymer utilization at 0.88% and amino acid utilization at 14.5%. In contrast, *B. mobilis* disproportionately utilized carboxylic and acetic acids (52.26%) and amines/amides (11.32%), compared to *C. campinensis* at 13.62% and 0.14% respectively (Table 3).

In silico identification of ARGs found in *Bacillus mobilis* and *Cupriavidus campinensis*

Antibiotic susceptibility testing of *B. mobilis* using the GPALL1F panel revealed resistance to 15 of the 23 antibiotics tested, corresponding to a 65.2% overall resistance rate, with susceptibility maintained for 34.8% of the agents. CARD-based resistome analysis identified 15 resistance determinants, with high-confidence ("perfect") matches comprising 46.7%, strict hits 26.7%, and loose hits 26.7% of the predictions (Figure 6a). Mechanistically, resistance was primarily mediated by target alteration (53.3%), followed by antibiotic inactivation (33.3%), efflux (13.3%), and target replacement (6.7%) (Figure 6c). Notably, key resistance genes included *mecA* (methicillin resistance, MRSA-like phenotype), *cfr* (linezolid resistance, oxazolidinone class), and rpoB (rifampicin resistance), mprF (daptomycin resistance, lipopeptides). A multidrug-resistant profile was evident, with complete resistance across the beta-lactam class (e.g., *blaZ*, *mecA*), fluoroquinolones (*gyrA*, *parC*), macrolide-lincosamide antibiotics (*ermB*, *ermC*), and tetracyclines (*tetK*, *tetL*) (Figure 6c). A detailed listing of the individual ARGs identified in *B. mobilis* is shown in Supplementary Table S2.

Antibiotic resistance profiling of C. *campinensis* revealed a clinically significant carbapenem-resistant Enterobacterales (CRE)-like profile. Phenotypic testing using the GN4F panel indicated resistance to 11 of 24 antibiotics (45.8%), including complete resistance to all three tested carbapenems (ertapenem, meropenem, doripenem), and susceptibility to 12 agents (50%). CARD-RGI analysis identified 27 resistance genes, with high-confidence matches (perfect hits) comprising 22.2%, strict hits 44.4%, and loose hits 33.3% (Figure 6b). Mechanistically, resistance was primarily mediated by Antibiotic Inactivation (63%), followed by Target Alteration (14.8%), efflux pump (14.8%), and target protection (7.4%) (Figure 6d; Supplementary Table S2). High-risk carbapenemase genes included *blaKPC-2* (ertapenem resistance, Class A), blaNDM-1 (meropenem resistance, Class B), blaVIM-2 (imipenem, meropenem, and ertapenem resistance) and *blaOXA-48* (doripenem resistance, Class D), each identified with strict to perfect confidence. Additional beta-lactam resistance genes such as *blaTEM-1, blaCTX-M, blaSHV-1,* and *blaAmpC* contributed to extensive resistance against penicillins and cephalosporins (Figure 6d). A detailed listing of the individual ARGs identified in *C. campinensis* is shown in Supplementary Table S3.

Discussion

In this study, the bacterial species *B. mobilis* and *C. campinensis* were isolated from cadmium-amended soil with Cd^{2+} levels approximately one order of magnitude higher than those typically found in soils highly contaminated with Cd^{2+}. This categorizes them as Cd^{2+} tolerant bacterial species, indicating their remarkable ability to survive in high Cd^{2+} concentrations.

C. campinensis (basionym: *R. campinensis*) was initially isolated from various heavy metal-contaminated industrial biotopes in Campine, northeastern Belgium (Goris et al., 2001), and from a heavy metal-contaminated playground in Salgótarján, Hungary (Abbaszade et al., 2020), demonstrating its adaptation and resistance to environmental stresses. Abbaszade et al. (2020) documented several typical metal-resistant genes and gene clusters in *C. campinensis* strain S14E4C, including *cadA* (cadmium-translocating P-type ATPase), *czcB* (cobalt-zinc-cadmium efflux RND transporter, membrane fusion protein), *czcR* (cobalt-zinc-cadmium resistance protein), among others. The *B. mobilis strain MCCC 1A05942* was isolated from sediment of the Indian Ocean (Liu et al., 2017) and a closely related strain *B. mobilis* CR3 strain isolated from Cr-polluted soil sample in Qinghai, China, can remove Cr(VI) mainly through bio-reduction by reductase (Ye et al., 2024). Various reductase enzymes are involved in heavy metal reduction (Ojha et al., 2023) and APS reductase was shown to be efficient in immobilizing soil Cd^{2+} in cadmium-contaminated paddy soils (Liu et al., 2024). The identification and characterization of these Cd^{2+}-tolerant bacterial strains highlight their potential use in the remediation of heavy metal-contaminated environments. Their ability to thrive in extreme conditions suggests they could be pivotal in developing biotechnological applications for the detoxification of cadmium-polluted soils. Additionally, understanding the genetic mechanisms underlying their resistance offers valuable insights for engineering more robust microbial strains for environmental clean-up strategies.

In recent years, a few microorganisms with the potential to absorb Cd^{2+} with varying efficiencies and limitations have been documented. For instance, *Pseudomonas aeruginosa* has been highlighted as a versatile microbe and a suitable biosorbent for the removal of Cd^{2+}. It also promotes plant growth and enhances heavy metal accumulation by plants (Chellaiah, 2018). Additionally, *Bacillus cereus*, when associated with lawn plants, showed approximately 33% removal efficiency of Cd^{2+} from contaminated soil (Zhou et al., 2024). *Rhizobium*

leguminosarum forms a symbiotic relationship with legumes, reducing Cd^{2+} toxicity in plants and potentially enhancing Cd^{2+} uptake and sequestration (Jach et al., 2022). *Klebsiella planticola* strain was shown to convert S_2O_3 into H_2S and precipitates Cd ions as insoluble sulfides (Kour et al., 2021). Additionally, in agricultural applications, *Bacillus subtilis* has been shown to promote plant growth and Cd^{2+} uptake in host plants, assisting phytoremediation processes by altering soil conditions to make Cd^{2+} more bioavailable (Li et al., 2022). Despite the promising strategy of bioremediation through microbial activity, the known versatile Cd^{2+}resistant bacteria remain limited. Therefore, we recommend that the potential of Cd^{2+} tolerant bacterial strains *B. mobilis* and *C. campinensis* in this study should be explored for their effectiveness in Cd^{2+} bioremediation, potentially contributing to innovative solutions for soil contamination.

It is not surprising that these Cd-tolerant species utilized limited substrates needed for growth in extreme environments and might devote energy to producing resistance determinants allowing them to live in extreme environments. The results showed that both bacterial strains can metabolize a low variety of carbon substrates with different efficiencies, reflecting their ability to thrive in environments with limited nutrient availability. Such metabolic flexibility is critical for bacteria inhabiting heavy metal-contaminated soils, where nutrient sources may be limited or irregular. *B. mobilis* exhibited high metabolic activity when exposed to substrates like pyruvic acid methyl ester (carbohydrate), D-malic acid, Itaconic acid, D-Galactonic acid γ-Lactone (carboxylic and acetic acids) and phenylethylamine (amine/amides), suggesting that *B. mobilis* can efficiently utilize for instance both simple carbohydrates (itaconic acid) and more complex carbon substrates (Phenylethylamine, D-Galactonic acid γ-Lactone). The significantly utilized substrates for *C. campinensis* were complex polymers (Tween-40 and Tween-80), an amino acid (L. Asparagine), and a simple carbohydrate (pyruvic acid methyl ester).

Microbial metabolism of specific carbon substrates plays a critical role in shaping community responses to heavy metal stress, as these substrates can influence both metal mobility and microbial tolerance mechanisms. Organic acids, amino acids, and surfactants have been linked to enhanced microbial activity, exopolysaccharide production, and increased solubility or uptake of metals in contaminated soils (Skorokhodova et al., 2021; Kenarova and Boteva, 2015; Memarian and Ramamurthy, 2013; Cheng et al., 2017; Harati et al., 2023). In this study, we found that *B. mobilis* and *C. campinensis* disproportionately utilized several carbon substrates under Cd^{2+} stress, and these utilization patterns are consistent with mechanisms previously linked to microbial remediation of heavy metals. For example, pyruvic acid and D-malic acid, which were among the most highly utilized substrates in our assays, are known to enhance microbial respiration and biomass production, as well as stimulate exopolysaccharide production that can immobilize heavy metals (Skorokhodova et al., 2021; Si et al., 2022; Adedayo et al., 2023; Lou et al., 2023). Similarly, itaconic acid and D-galactonic acid-γ-lactone, also strongly metabolized in our study, have been shown to promote the growth of metal-binding microbes and to support microbial resistance to heavy metals (Krishnamoorthy et al., 2021; Kenarova and Boteva, 2015; Martínez-Toledo et al., 2021). Our data further revealed that phenylethylamine and L-asparagine supported the growth of metal-tolerant taxa, in line with earlier reports connecting these substrates to contaminant degradation pathways and reductions in bioavailable Zn (Koner et al., 2022; Ghorbanzadeh et al., 2022). Finally, we observed notable utilization of surfactants such as Tween-40 and Tween-80, which studies have shown their role in enhancing the solubility and microbial uptake of polycyclic aromatic hydrocarbons and metals, including Cd^{2+} and Pb^{2+} (Dhenain et al., 2006; Lima et al., 2011; Memarian and Ramamurthy, 2013; Cheng et al., 2017; Harati et al., 2023). Collectively, these findings demonstrate that the substrate preferences identified in our isolates align with known biostimulation mechanisms and highlight their potential for enhancing Cd^{2+} uptake and reduction in contaminated soils.

Bioaugmentation and biostimulation are well-established strategies for accelerating the on-site degradation of organic pollutants and facilitating metal reduction. Introducing specific carbon substrates such as organic acids or surfactants can be crucial in promoting the activity of native, metal-tolerant microorganisms, among which particular species may enhance the rate and efficiency of bioremediation. In this context, the six carbon substrates identified as highly utilized by *B. mobilis* and the four substrates identified for *C. campinensis* represent promising carbon substrates for further investigation. The above findings provide a foundational characterization of the Cd^{2+}-tolerance and metabolic capacity of *B. mobilis* and *C. campinensis* for potential targeted biostimulation to boost *in-situ* bioremediation processes for heavy metals at contaminated sites. Although we did not evaluate their direct effects on plants under Cd^{2+} stress, evidence from related *Bacillus* and *Cupriavidus* strains suggests potential applicability in rhizosphere colonization, cadmium immobilization, and mitigation of metal-induced phytotoxicity (Chen et al., 2008; Rajkumar et al., 2010; Ma et al., 2016; Nayak et al., 2018; Yang et al., 2024). Future studies should specifically assess the plant-growth–promoting and stress-alleviating capacities of these isolates in cadmium-contaminated soils.

The dynamic effects of antibiotics on *B. mobilis* and *C. campinensis* growth patterns, as observed in this study, provide critical insights into how bacterial isolates from cadmium-amended soils respond to diverse antibiotic pressures. These results reveal significant differences in growth phases and rates, reflecting varying degrees of susceptibility and adaptive responses. Heavy metals like $Cd^{2+}$are known to co-select for antibiotic resistance, as resistance genes often co-localize with metal resistance determinants on mobile genetic elements such as plasmids and transposons (Pal et al., 2015). This co-selection could explain the elevated baseline resistance observed in *B. mobilis* and *C. campinensis*, especially to antibiotics with overlapping resistance mechanisms, such as beta-lactams and aminoglycosides.

For *C. campinensis*, most tested antibiotics, including imipenem, tigecycline, tetracycline, gentamicin, levofloxacin, and ceftriaxone, were inhibitory at all concentrations. However, notable exceptions, such as the recovery of growth at low ceftriaxone concentrations (0.5 μg/mL), suggest concentration-dependent adaptation mechanisms. The extended lag phase observed at higher antibiotic concentrations, such as those of piperacillin and doripenem, likely represents a survival strategy allowing cells to endure sublethal antibiotic stress before resuming growth. Such lag phase extensions may involve upregulation of efflux pumps, stress response pathways, or the activation of antibiotic resistance genes, as

previously described in resistant bacteria (Lambert, 2002; Baker-Austin et al., 2006; Martinez, 2009).

In contrast, *B. mobilis* exhibited greater resilience, with nearly 50% of tested antibiotics showing limited activity across all concentrations. This limited susceptibility could be attributed to intrinsic resistance mechanisms or the physiological robustness of *B. mobilis* under stress conditions. Notably, antibiotics such as erythromycin, clindamycin, daptomycin, ampicillin, and vancomycin were ineffective, with growth dynamics comparable to antibiotic-free controls. These observations are consistent with reports that Gram-positive bacteria, particularly environmental isolates, often possess structural barriers, such as thick peptidoglycan layers, and constitutive efflux pumps that confer broad-spectrum resistance (Baker-Austin et al., 2006; Martinez, 2009). The distinct growth patterns observed for levofloxacin, nitrofurantoin, ciprofloxacin, and streptomycin highlight the complexity of antibiotic concentration-dependent effects. For instance, *B. mobilis* exposed to levofloxacin exhibited an extended lag phase of up to 48 h at 1 μg mL^{-1}, followed by gradual growth, whereas above 2 μg mL^{-1} there was complete inhibitory effect. This prolonged lag phase may indicate the activation of DNA repair systems, as levofloxacin targets bacterial DNA gyrase (Table 2), inducing double-strand breaks that necessitate extensive repair before replication can resume (Hooper and Jacoby, 2015). Similarly, the delayed growth of cells exposed to streptomycin underscores the potential for ribosomal protein modification or aminoglycoside inactivation enzymes to mitigate translational inhibition (Davies and Davies, 2010).

Our *in silico* analyses revealed comprehensive multidrug resistance (MDR) profiles in both strains, complementing their high Cd^{2+}-tolerance; a hallmark of *C. campinensis* noted in other strains tolerating Cd levels up to ~19 mM (Abbaszade et al., 2020). *B. mobilis* exhibited a broad ARG burden, including β-lactamases (*blaZ*, *mecA*), fluoroquinolone targets (*gyrA*, *parC*), macrolide-clindamycin methylases (*ermB*, *ermC*), and tetracycline efflux pumps (*tetK*, *tetL*). Such a profile reflects its environmental adaptability and may point to horizontal gene transfer from commensals or pathogens (Baker-Austin et al., 2006). The presence of *mprF* highlights its capacity to resist lipopeptide antibiotics like daptomycin (Thitiananpakorn et al., 2020), underlining the need for caution when considering its use in bioremediation.

Similarly, *C. campinensis* displayed a clinically alarming resistome profile, defined by strict to perfect matches to *blaKPC-2*, *blaNDM-1*, blaVIM-2, and *blaOXA-48*. These enzymes confer resistance to all tested carbapenems and are recognized as high-risk carbapenemase globally (Jean et al., 2022). Class A–D β-lactamases were well-represented, aligning with previously observed intrinsic resistome signatures in *Cupriavidus*. The detection of RND family efflux pumps -key mediators of broad-spectrum resistance-further underscores their potential clinical threat (Anes et al., 2015).

A particularly significant finding of this study is the persistence of growth effects well beyond the standard 24-h incubation period used in most clinical and environmental susceptibility testing protocols (CLSI, 2023). For example, in *C. campinensis*, antibiotics such as ceftriaxone, piperacillin, and ampicillin exhibited delayed inhibitory effects or adaptive growth after extended lag phases of 36–50 h. Similarly, in *B. mobilis*, lag phases of up to 48 h for ciprofloxacin and 30 h for nitrofurantoin reveal the potential for delayed bacterial adaptation to antibiotic stress. The lack of complete inhibition at higher concentrations highlights the potential for resistance mechanisms to confer partial protection, even under substantial antibiotic stress. These observations suggest that traditional susceptibility testing methods, which typically assess growth inhibition within 24 h, may overlook critical adaptive responses and underestimate the resilience of certain bacterial isolates. Extending susceptibility testing beyond the standard 24-h timeframe is crucial for understanding the full spectrum of bacterial responses to antibiotics (Theophel et al., 2014). Delayed growth recovery, as observed in this study, could have significant implications for treatment efficacy and the emergence of resistance. For instance, patients receiving antibiotics may initially appear to respond to treatment, but delayed bacterial recovery could lead to treatment failure or relapse. Additionally, sublethal antibiotic exposure during prolonged lag phases might facilitate the development of tolerance or resistance through selection of adaptive mutants or the activation of stress-induced resistance mechanisms (Theophel et al., 2014; Drawz and Bonomo, 2010). Ecologically, in contaminated ecosystems such as cadmium-amended soils, bacterial isolates are likely subjected to prolonged exposure to sublethal antibiotic concentrations due to environmental persistence of antibiotics and heavy metal co-selection pressures. The extended lag phases observed in this study could represent an ecologically relevant adaptation, allowing bacteria to survive fluctuating antibiotic concentrations. This highlights the need for susceptibility testing protocols that reflect environmental conditions more accurately, particularly in ecosystems where co-selection for antibiotic and metal resistance is likely (Baker-Austin et al., 2006; Pal et al., 2015).

Our findings emphasize the importance of dynamic, time-resolved assessments of bacterial growth in both clinical and environmental contexts. Automated OD measurements, as implemented in this study, provide a valuable tool for capturing differential growth dynamics and resistance profiles of *B. mobilis* and *C. campinensis* over extended time periods, offering a more comprehensive understanding of bacterial responses to antibiotics. Future studies should explore the molecular mechanisms underlying extended lag phases and delayed growth recovery, particularly in relation to heavy metal stress and resistance gene expression.

Conclusion

This study identified *B. mobilis* and *C. campinensis* as multidrug resistant and cadmium-tolerant bacteria with potential for bioremediation of heavy metal-contaminated soils. Both strains exhibited limited substrate utilization profiles, indicative of metabolic adaptations for survival in nutrient-poor, metal-stressed environments. Their ability to metabolize key substrates, such as organic acids and surfactants, supports their role in enhancing heavy metal bioavailability and mobilization in contaminated soils. Antibiotic susceptibility testing revealed delayed growth responses beyond the standard 24-h timeframe, highlighting the limitations of traditional testing protocols in capturing adaptive resistance mechanisms. We summarize predicted resistance genes *in silico* from available genomic data entered in CARD-RGI. Using a higher ARG-target coverage cutoff (>95%) predicted presence of seven and six perfect hits in *B. mobilis* and *C. campinensis* respectively. *C. campinensis* exhibited critical resistance to all tested carbapenems

revealing a concerning carbapenem-resistant Enterobacteriaceae (CRE) profile. These findings underscore the ecological relevance of extended testing periods, particularly in environments where co-selection pressures from heavy metals and antibiotics persist. Also, the observed co-selection of resistance to both $Cd^{2+}$and antibiotics further underscores the ecological complexity of contaminated environments, where heavy metal pressures and residual antibiotic concentrations may synergistically drive resistance evolution. Our study demonstrates that *B. mobilis* and *C. campinensis* isolated from cadmium-spiked soils exhibit both functional diversity in carbon metabolism and multidrug resistance traits, underscoring their ability to adapt and persist under high Cd^{2+} stress. These findings highlight the potential of these strains as candidates for application in bioremediation of heavy metal–contaminated environments, where metabolic versatility and resistance determinants are critical for survival and ecological function. While additional studies could further elucidate the genetic pathways underlying these traits, the present work provides clear evidence of their ecological resilience and biotechnological promise.

Data availability statement

The original contributions presented in the study are included in the article/Supplementary Material, further inquiries can be directed to the corresponding author.

Author contributions

PA: Project administration, Writing – review and editing, Formal Analysis, Investigation, Methodology, Writing – original draft, Funding acquisition, Supervision, Software, Data curation, Conceptualization, Resources. EJ: Methodology, Investigation, Writing – review and editing, Resources. NS: Methodology, Writing – review and editing, Investigation.

Funding

The author(s) declare that financial support was received for the research and/or publication of this article. This work was partly funded by generous support from the J. William Asher and Melanie J. Norton Endowed Fund in the Sciences, DePauw University, Greencastle, IN.

Acknowledgments

We thank Kennett Brown of Department of Geology and Environmental Geosciences, DePauw University, Greencastle, IN for metal analysis of the amended soil. Jenni McGaughey of the Biology Department at DePauw, helped with laboratory logistics and support.

Conflict of interest

The authors declare that the research was conducted in the absence of any commercial or financial relationships that could be construed as a potential conflict of interest.

Generative AI statement

The author(s) declare that Generative AI was used in the creation of this manuscript. Generative AI was employed to assist in debugging and optimizing Python-integrated scripts used for CARD Antibiotic Resistance Ontology sunburst classification.

Any alternative text (alt text) provided alongside figures in this article has been generated by Frontiers with the support of artificial intelligence and reasonable efforts have been made to ensure accuracy, including review by the authors wherever possible. If you identify any issues, please contact us.

Publisher's note

Supplementary material

The Supplementary Material for this article can be found online at: https://www.frontiersin.org/articles/10.3389/fenvs.2025.1668462/full#supplementary-material

References

Abbas, S., Zulfiqar, S., Arshad, M., Khalid, N., Hussain, A., and Ahmed, I. (2025). Molecular characterization of heavy metal-tolerant bacteria and their potential for bioremediation and plant growth promotion. *Front. Microbiol.* 16, 1644466. Advance online publication. doi:10.3389/fmicb.2025.1644466

Abbaszade, G., Szabó, A., Vajna, B., Farkas, R., Szabó, C., and Tóth, E. (2020). Whole genome sequence analysis of Cupriavidus campinensis S14E4C, a heavy metal resistant bacterium. *Mol. Biol. Rep.* 47, 3973–3985. doi:10.1007/s11033-020-05490-8

Adedayo, A. A., Fadiji, A. E., and Babalola, O. O. (2023). Quantifying the respiratory pattern of rhizosphere microbial communities in healthy and diseased tomato plants using carbon substrates. *J. Soil Sci. Plant Nutr.* 23 (4), 6485–6496. doi:10.1007/s42729-023-01504-z

Akinwole, P. O., Shaffer, N. G., Pasini, C. Z., Carr, K. M., Brown, K. L., and Owojori, O. J. (2024). Ecotoxicity evaluation using the avoidance response of the oribatid mite Oppia nitens (acari: Oribatida) in bioplastics, microplastics, and contaminated Superfund field sites. *Chemosphere* 359, 142301. doi:10.1016/j.chemosphere.2024.142301

Alcock, B. P., Huynh, W., Chalil, R., Smith, K. W., Raphenya, A. R., Wlodarski, M. A., et al. (2023). CARD 2023: expanded curation, support for machine learning, and resistome prediction at the Comprehensive Antibiotic Resistance Database. *Nucleic acids Res.* 51 (D1), D690–D699. doi:10.1093/nar/gkac920

Anes, J., McCusker, M. P., Fanning, S., and Martins, M. (2015). The ins and outs of RND efflux pumps in Escherichia coli. *Front. Microbiol.* 6, 587. doi:10.3389/fmicb.2015.00587

Arce-Inga, M., González-Pérez, A. R., Hernandez-Diaz, E., Chuquibala-Checan, B., Chavez-Jalk, A., Llanos-Gomez, K. J., et al. (2022). Bioremediation potential of native Bacillus sp. strains as a sustainable strategy for cadmium accumulation of theobroma cacao in Amazonas region. *Microorganisms* 10 (11), 2108. doi:10.3390/microorganisms10112108

Baker-Austin, C., Wright, M. S., Stepanauskas, R., and McArthur, J. V. (2006). Co-selection of antibiotic and metal resistance. *Trends Microbiol.* 14 (4), 176–182. doi:10.1016/j.tim.2006.02.006

Bi, X. Y., Feng, X. B., Yang, Y. G., Qiu, G. L., and Lia, G. H. (2006). Quantitative assessment of cadmium emission from zinc smelting and its influences on the surface soils and mosses in Hezhang County, Southwestern China. *Atmos. Environ.* 40, 4228–4233. doi:10.1016/j.atmosenv.2006.02.019

Bisong, E. (2019). *Building machine learning and deep learning models on Google cloud platform*. Berkeley, CA, USA: Apress.

Bravo, D., and Braissant, O. (2022). Cadmium-tolerant bacteria: current trends and applications in agriculture. *Lett. Appl. Microbiol.* 74 (3), 311–333. doi:10.1111/lam.13594

Cattani, I., Zhang, H., Beone, G. M., Del Re, A. A. M., Boccelli, R., and Trevisan, M. (2009). The role of natural purified humic acids in modifying mercury accessibility in water and soil. *J. Environ. Qual.* 38 (2), 493–501. doi:10.2134/jeq2008.0175

Chellaiah, E. R. (2018). Cadmium (heavy metals) bioremediation by Pseudomonas aeruginosa: a minireview. *Appl. Water Sci.* 8 (6), 154. doi:10.1007/s13201-018-0796-5

Chen, W. M., Wu, C. H., James, E. K., and Chang, J. S. (2008). Metal biosorption capability of Cupriavidus taiwanensis and its effects on heavy metal removal by nodulated Mimosa pudica. *J. Hazard. Mater.* 151 (2-3), 364–371. doi:10.1016/j.jhazmat.2007.05.082

Cheng, M., Zeng, G., Huang, D., Yang, C., Lai, C., Zhang, C., et al. (2017). Advantages and challenges of Tween 80 surfactant-enhanced technologies for the remediation of soils contaminated with hydrophobic organic compounds. *Chem. Eng. J.* 314, 98–113. doi:10.1016/j.cej.2016.12.135

Clemens, S. (2006). Toxic metal accumulation, responses to exposure and mechanisms of tolerance in plants. *Biochimie* 88 (11), 1707–1719. doi:10.1016/j.biochi.2006.07.003

Clinical and Laboratory Standards Institute [CLSI] (2023). *Performance standards for antimicrobial susceptibility testing*. 33rd ed. Wayne, PA: Clinical and Laboratory Standards Institute.

Davies, J., and Davies, D. (2010). Origins and evolution of antibiotic resistance. *Microbiol. Mol. Biol. Rev.* 74 (3), 417–433. doi:10.1128/mmbr.00016-10

Dhenain, A., Mercier, G., Blais, J. F., and Bergeron, M. (2006). PAH removal from black sludge from aluminium industry by flotation using non-ionic surfactants. *Environ. Technol.* 27 (9), 1019–1030. doi:10.1080/09593332708618716

Diels, L., Dong, Q. H., van der Lelie, D., Baeyens, W., and Mergeay, M. (1995). The czc operon of Alcaligenes eutrophus CH34: from resistance mechanism to the removal of heavy metals. *J. Ind. Microbiol.* 14, 142–153. doi:10.1007/bf01569896

Drawz, S. M., and Bonomo, R. A. (2010). Three decades of β-lactamase inhibitors. *Clin. Microbiol. Rev.* 23 (1), 160–201. doi:10.1128/cmr.00037-09

Forsberg, K. J., Reyes, A., Wang, B., Selleck, E. M., Sommer, M. O., and Dantas, G. (2012). The shared antibiotic resistome of soil bacteria and human pathogens. *Science* 337 (6098), 1107–1111. doi:10.1126/science.1220761

Ghorbanzadeh, N., Ghanbari, Z., Farhangi, M. B., and Rad, M. K. (2022). Zinc bioremediation in soil by two isolated L-asparaginase and urease producing bacteria strains. *Appl. Geochem* 140, 105271. doi:10.1016/j.apgeochem.2022.105271

Goris, J., De Vos, P., Coenye, T., Hoste, B., Janssens, D., Brim, H., et al. (2001). Classification of metal-resistant bacteria from industrial biotopes as Ralstonia campinensis sp. nov., Ralstonia metallidurans sp. nov. and Ralstonia basilensis Steinle et al. 1998 emend. *Int. J. Syst. Evol. Microbiol.* 51 (Pt 5), 1773–1782. doi:10.1099/00207713-51-5-1773

Harati, M., Gharibzadeh, F., Moradi, M., and Kalantary, R. R. (2023). Remediation of phenanthrene and cadmium co-contaminated soil by using a combined process including soil washing and electrocoagulation. *Int. J. Environ. Anal. Chem.* 103 (19), 7811–7829. doi:10.1080/03067319.2021.1976168

Harch, B. D., Correll, R. L., Meech, W., Kirkby, C. A., and Pankhurst, C. E. (1997). Using the Gini coefficient with BIOLOG substrate utilisation data to provide an alternative quantitative measure for comparing bacterial soil communities. *J. Microbiol. Methods* 30 (1), 91–101. doi:10.1016/s0167-7012(97)00048-1

Hawal, L. H., Al-Sulttani, A. O., and Hamza, J. N. (2023). Cadmium removal from contaminated soil by electro-kinetic method. *J. Ecol. Eng.* 24 (1), 79–86. doi:10.12911/22998993/156007

Hooper, D. C., and Jacoby, G. A. (2015). Mechanisms of drug resistance: quinolone resistance. *Ann. N. Y. Acad. Sci.* 1354 (1), 12–31. doi:10.1111/nyas.12830

Huang, H., Jia, Y., Sun, G. X., and Zhu, Y. G. (2012). Arsenic speciation and volatilization from flooded paddy soils amended with different organic matters. *Environ. Sci. Technol.* 46 (4), 2163–2168. doi:10.1021/es203635s

Jach, M. E., Sajnaga, E., and Ziaja, M. (2022). Utilization of legume-nodule bacterial symbiosis in phytoremediation of heavy metal-contaminated soils. *Biology* 11 (5), 676. doi:10.3390/biology11050676

Jarup, L., Berglund, M., Elinder, C. G., Nordberg, G., and Vahter, M. (1998). Health effects of cadmium exposure–a review of the literature and a risk estimate. *Scand. J. Work Environ. Health* 24 (Suppl. 1), 1–51. Available online at: https://pubmed.ncbi.nlm.nih.gov/9569444/.

Jean, S. S., Harnod, D., and Hsueh, P. R. (2022). Global threat of carbapenem-resistant gram-negative bacteria. *Front. Cell. Infect. Microbiol.* 12, 823684. doi:10.3389/fcimb.2022.823684

Jorgensen, J. H., and Ferraro, M. J. (2009). Antimicrobial susceptibility testing: a review of general principles and contemporary practices. *Clin. Infect. Dis.* 49, 1749–1755. doi:10.1086/647952

Kabata-Pendias, A. (2010). Trace elements in soils and plants. In *Trace elements in soils and plants fourth edition*; Kabata-Pendias, A., Ed.; Boca Raton, FL, USA: CRC Press (Taylor and Francis Group).

Kenarova, A., and Boteva, S. (2015). "Functional diversity of microorganisms in heavy metal-polluted soils," in *Heavy metal contamination of soils: monitoring and remediation*, 245–257.

Koner, S., Chen, J. S., Hsu, B. M., Rathod, J., Huang, S. W., Chien, H. Y., et al. (2022). Depth-resolved microbial diversity and functional profiles of trichloroethylene-contaminated soils for Biolog EcoPlate-based biostimulation strategy. *J. Hazard Mater* 424, 127266. doi:10.1016/j.jhazmat.2021.127266

Kour, D., Kaur, T., Devi, R., Yadav, A., Singh, M., Joshi, D., et al. (2021). Beneficial microbiomes for bioremediation of diverse contaminated environments for environmental sustainability: present status and future challenges. *Environ. Sci. Pollut. Res. Int.* 28, 24917–24939. doi:10.1007/s11356-021-13252-7

Krishnamoorthy, S., Ramakrishnan, G., and Dhandapani, B. (2021). Recovery of valuable metals from waste printed circuit boards using organic acids synthesised by Aspergillus niveus. *IET Nanobiotechnol* 15 (2), 212–220. doi:10.1049/nbt2.12001

Kubier, A., Wilkin, R. T., and Pichler, T. (2019). Cadmium in soils and groundwater: a review. *Appl. Geochem* 108, 104388. doi:10.1016/j.apgeochem.2019.104388

Lambert, P. (2002). Mechanisms of antibiotic resistance in Pseudomonas aeruginosa. *JRSM* 95 (Suppl. 41), 22–26.

Lata, S., Mishra, T., and Kaur, S. (2021). Cadmium bioremediation potential of bacillus sp. and cupriavidus sp. *J. Pure Appl. Microbiol.* 15 (3), 1665–1680. doi:10.22207/jpam.15.3.63

Lee, S., Lee, J., Choi, Y. J., and Kim, J. (2009). *In situ* stabilization of cadmium-lead- and zinc-contaminated soil using various amendments. *Chemosphere* 77 (8), 1069–1075. doi:10.1016/j.chemosphere.2009.08.056

Li, Q., Xing, Y., Huang, B., Chen, X., Ji, L., Fu, X., et al. (2022). Rhizospheric mechanisms of Bacillus subtilis bioaugmentation-assisted phytostabilization of cadmium-contaminated soil. *Sci. Total Environ.* 825, 154136. doi:10.1016/j.scitotenv.2022.154136

Lima, A. T., Kleingeld, P. J., Heister, K., and Loch, J. G. (2011). Removal of PAHs from contaminated clayey soil by means of electro-osmosis. *Sep. Purif. Technol.* 79 (2), 221–229. doi:10.1016/j.seppur.2011.02.021

Liu, Y., Du, J., Lai, Q., Zeng, R., Ye, D., Xu, J., et al. (2017). Proposal of nine novel species of the Bacillus cereus group. *Int. J. Syst. Evol. Microbiol.* 67 (8), 2499–2508. doi:10.1099/ijsem.0.001821

Liu, L., Li, W., Song, W., and Guo, M. (2018). Remediation techniques for heavy metal-contaminated soils: principles and applicability. *Sci. Total Environ.* 633, 206–219. doi:10.1016/j.scitotenv.2018.03.161

Liu, Y., Xu, Y., Qin, X., Zhao, L., Huang, Q., and Wang, L. (2019). Effects of water and organic manure coupling on the immobilization of cadmium by sepiolite. *J. Soils Sediments* 19, 798–808. doi:10.1007/s11368-018-2081-5

Liu, Z., Li, Y., Shan, S., Zhang, M., Yang, H., Cheng, W., et al. (2024). Regulatory roles of APS reductase in Citrobacter sp. XT1-2-2 as a response mechanism to cadmium immobilization in rice. *Ecotoxicol. Environ. Saf.* 284, 116892. doi:10.1016/j.ecoenv.2024.116892

Lombi, E., Hamon, R. E., McGrath, S. P., and McLaughlin, M. J. (2003). Lability of Cd, Cu, and Zn in polluted soils treated with lime, beringite, and red mud and identification of a non-labile colloidal fraction of metals using isotopic techniques. *Environ. Sci. Technol.* 37 (5), 979–984. doi:10.1021/es026083w

Lou, Z., Zheng, X., Bede, D., Dai, W., Wan, C., Wang, H., et al. (2023). New perspectives for mechanisms, ingredients, and their preparation for promoting the formation of beneficial bacterial biofilm. *J. Food Meas. Charact.* 17 (3), 2386–2403. doi:10.1007/s11694-022-01777-5

Ma, Y., Oliveira, R. S., Freitas, H., and Zhang, C. (2016). Biochemical and molecular mechanisms of plant-microbe-metal interactions: relevance for phytoremediation. *Front. plant Sci.* 7, 918. doi:10.3389/fpls.2016.00918

Martinez, J. L. (2009). Environmental pollution by antibiotics and by antibiotic resistance determinants. *Environ. Pollut.* 157 (11), 2893–2902. doi:10.1016/j.envpol.2009.05.051

Martínez-Toledo, Á., González-Mille, D. J., García-Arreola, M. E., Cruz-Santiago, O., Trejo-Acevedo, A., and Ilizaliturri-Hernández, C. A. (2021). Patterns in utilization of carbon sources in soil microbial communities contaminated with mine solid wastes from San Luis Potosi, Mexico. *Ecotoxicol. Environ. Saf.* 208, 111493. doi:10.1016/j.ecoenv.2020.111493

McArthur, J. V., and Tuckfield, R. C. (2000). Spatial patterns in antibiotic resistance among stream bacteria: effects of industrial pollution. *Appl. Environ. Microbiol.* 66, 3722–3726. doi:10.1128/aem.66.9.3722-3726.2000

McLaughlin, M. J., and Singh, B. R. (1999). *Cadmium in soils and plants*. Norway, Norway: Kluwer Academic Publishers. Agricultural University of. doi:10.1007/978-94-011-4473-5

Memarian, R., and Ramamurthy, A. S. (2013). Modeling of lead and cadmium uptake by plants in the presence of surfactants. *Environ. Monit. Assess.* 185 (3), 2067–2071. doi:10.1007/s10661-012-2688-8

Nayak, A. K., Panda, S. S., Basu, A., and Dhal, N. K. (2018). Enhancement of toxic Cr (VI), Fe, and other heavy metals phytoremediation by the synergistic combination of native Bacillus cereus strain and Vetiveria zizanioides L. *Int. J. phytoremediation* 20 (7), 682–691. doi:10.1080/15226514.2017.1413332

Nnaji, N. D., Anyanwu, C. U., Miri, T., and Onyeaka, H. (2024). Mechanisms of heavy metal tolerance in bacteria: a review. *Sustainability* 16 (24), 11124. doi:10.3390/su162411124

Ojha, A., Jaiswal, S., Thakur, P., and Mishra, S. K. (2023). Bioremediation techniques for heavy metal and metalloid removal from polluted lands: a review. *Int. J. Environ. Sci. Technol.* 20 (9), 10591–10612. doi:10.1007/s13762-022-04502-3

Pal, C., Bengtsson-Palme, J., Kristiansson, E., and Larsson, D. J. (2015). Co-occurrence of resistance genes to antibiotics, biocides and metals reveals novel insights into their co-selection potential. *BMC genomics* 16, 964–14. doi:10.1186/s12864-015-2153-5

Pandey, B., Kinrade, S. D., and Catalan, L. J. J. (2012). Effects of carbonation on the leachability and compressive strength of cement-solidified and geopolymer-solidified synthetic metal wastes. *J. Environ. Manage* 101, 59–67. doi:10.1016/j.jenvman.2012.01.029

Park, J. H., Lamb, D., Paneerselvam, P., Choppala, G., Bolan, N., and Chung, J. W. (2011). Role of organic amendments on enhanced bioremediation of heavy metal (loid) contaminated soils. *J. Hazard Mater* 185 (2-3), 549–574. doi:10.1016/j.jhazmat.2010.09.082

Qattan, S. Y. A. (2025). Harnessing bacterial consortia for effective bioremediation: targeted removal of heavy metals, hydrocarbons, and persistent pollutants. *Environ. Sci. Eur.* 37, 85. doi:10.1186/s12302-025-01103-y

Rajkumar, M., Ae, N., Prasad, M. N. V., and Freitas, H. (2010). Potential of siderophore-producing bacteria for improving heavy metal phytoextraction. *Trends Biotechnol.* 28 (3), 142–149. doi:10.1016/j.tibtech.2009.12.002

Salt, D. E., Blaylock, M., Kumar, N. P., Dushenkov, V., Ensley, B. D., Chet, I., et al. (1995). Phytoremediation: a novel strategy for the removal of toxic metals from the environment using plants. *Nat. Biotechnol.* 13 (5), 468–474. doi:10.1038/nbt0595-468

Sánchez-Castro, I., Molina, L., Prieto-Fernández, M., and Segura, A. (2023). Past, present and future trends in the remediation of heavy-metal contaminated soil - remediation techniques applied in real soil-contamination events. *Heliyon* 9 (6), e16692. doi:10.1016/j.heliyon.2023.e16692

Seiler, C., and Berendonk, T. U. (2012). Heavy metal driven co-selection of antibiotic resistance in soil and water bodies impacted by agriculture and aquaculture. *Front. Microbiol.* 3, 399. doi:10.3389/fmicb.2012.00399

Si, P., Shao, W., Yu, H., Xu, G., and Du, G. (2022). Differences in microbial communities stimulated by malic acid have the potential to improve nutrient absorption and fruit quality of grapes. *Front. Microbiol.* 13, 850807. doi:10.3389/fmicb.2022.850807

Simmer, R. A., and Schnoor, J. L. (2022). Phytoremediation, bioaugmentation, and the plant microbiome. *Environ. Sci. Technol.* 56 (23), 16602–16610. doi:10.1021/acs.est.2c05970

Skorokhodova, A. Y., Gulevich, A. Y., and Debabov, V. G. (2021). Optimization of the anaerobic production of pyruvic acid from glucose by recombinant escherichia coli strains with impaired fermentation ability *via* enforced atp hydrolysis. *Appl. Biochem. Microbiol.* 57, 434–442. doi:10.1134/s0003683821040153

Sreedevi, P. R., Suresh, K., and Jiang, G. (2022). Bacterial bioremediation of heavy metals in wastewater: a review of processes and applications. *J. Water Process Eng.* 48, 102884. doi:10.1016/j.jwpe.2022.102884

Stepanauskas, R., Glenn, T. C., Jagoe, C. H., Tuckfield, R. C., Lindell, A. H., McArthur, J. V., et al. (2006). Co-selection for microbial resistance to metals and antibiotics in freshwater microcosms. *Environ. Microbiol.* 8 (9), 1510–1514. doi:10.1111/j.1462-2920.2006.01091.x

Sun, Z., Zhao, M., Chen, L., Gong, Z., Hu, J., and Ma, D. (2023). Electrokinetic remediation for the removal of heavy metals in soil: limitations, solutions and prospection. *Sci. Total Environ.* 903, 165970. doi:10.1016/j.scitotenv.2023.165970

Theophel, K., Schacht, V. J., Schlüter, M., Schnell, S., Stingu, C. S., Schaumann, R., et al. (2014). The importance of growth kinetic analysis in determining bacterial susceptibility against antibiotics and silver nanoparticles. *Front. Microbiol.* 5, 544. doi:10.3389/fmicb.2014.00544

Thitiananpakorn, K., Aiba, Y., Tan, X. E., Watanabe, S., Kiga, K., Sato'o, Y., et al. (2020). Association of mprF mutations with cross-resistance to daptomycin and vancomycin in methicillin-resistant Staphylococcus aureus (MRSA). *Sci. Rep.* 10 (1), 16107. doi:10.1038/s41598-020-73108-x

United Nations Environment Programme (2010). Final review of scientific information on cadmium-version of December. Available online at: https://www.unep.org/resources/report/final-review-scientific-information-cadmium.

US EPA (2024). EPA's Web Archive. Washington, D.C.: Priority chemicals and fact sheets website. Available online at: https://archive.epa.gov/epawaste/hazard/wastemin/web/html/priority.html (Accessed February 22, 2016).

Voglar, G. E., and Lestan, D. (2010). Solidification/stabilisation of metals contaminated industrial soil from former Zn smelter in Celje, Slovenia, using cement as a hydraulic binder. *J. Hazard Mater* 178, 926–933. doi:10.1016/j.jhazmat.2010.02.026

Waalkes, M. P. (2000). Cadmium carcinogenesis in review. *J. Inorg. Biochem.* 79 (1-4), 241–244. doi:10.1016/s0162-0134(00)00009-x

Wagner-Döbler, I. (2003). Pilot plant for bioremediation of mercury-containing industrial wastewater. *Appl. Microbiol. Biotechnol.* 62 (2-3), 124–133. doi:10.1007/s00253-003-1322-7

Weber, K. P., and Legge, R. L. (2009). One-dimensional metric for tracking bacterial community divergence using sole carbon source utilization patterns. *J. Microbiol. Method* 79 (1), 55–61. doi:10.1016/j.mimet.2009.07.020

Yang, Y. K., Zhang, C., Shi, X. J., Tao, L. I. N., and Wang, D. Y. (2007). Effect of organic matter and pH on mercury release from soils. *J. Environ. Sci.* 19 (11), 1349–1354. doi:10.1016/s1001-0742(07)60220-4

Yang, Q., Liang, X. R., Wang, L., Yang, R. Y., He, C. Z., Tu, C. L., et al. (2024). Urease-producing bacteria with plant growth-promoting ability that may tolerate and remove cadmium from aqueous solution. *Int. J. Phytoremediation* 26 (12), 2010–2020. doi:10.1080/15226514.2024.2372445

Ye, Y., Hao, R., Shan, B., Zhang, J., Li, J., and Lu, A. (2024). Mechanism of Cr (VI) removal by efficient Cr (VI)-resistant Bacillus mobilis CR3. *World J. Microbiol. Biotechnol.* 40 (1), 21. doi:10.1007/s11274-023-03816-9

Zhang, N., Liu, W., Yang, H., Yu, X., Gutknecht, J. L., Zhang, Z., et al. (2013). Soil microbial responses to warming and increased precipitation and their implications for ecosystem C cycling. *Oecologia* 173 (3), 1125–1142. doi:10.1007/s00442-013-2685-9

Zhou, B., Yang, Z., Chen, X., Jia, R., Yao, S., Gan, B., et al. (2024). Microbiological mechanisms of collaborative remediation of cadmium-contaminated soil with bacillus cereus and lawn plants. *Plants* 13 (10), 1303. doi:10.3390/plants13101303